Animal studies

For inoculation into mice, BCG-Tokyo and BCG-ΔUT were cultured in Middlebrook 7H9 to log phase and stored at 10^8 CFU mL^{-1} at −80 °C. Before aliquots were used for inoculation, the concentration of viable bacilli was determined by plating cells on the Middlebrook 7H10 agar plate. Three 5-week-old C57BL/6J mice per group were inoculated intradermally with 0.1 mL phosphate-buffered saline (PBS) containing 1×10^2 or 1×10^3 BCG-Tokyo or BCG-ΔUT. The animals were kept under specific pathogen-free conditions and were supplied with sterilized food and water. Four weeks after injection, the spleens were removed, and the splenocytes were suspended at a concentration of 2×10^6 cells mL^{-1} in culture medium, and stimulated with the indicated concentration of BCC or MLM in triplicate in 96-well round-bottomed microplates. The individual culture supernatants were collected 3 days after stimulation, and IFN-γ and IL-2 were measured using an OptEIA mouse ELISA set.

Statistical analysis

The Student's *t*-test was applied to determine statistical differences.

Results

Induction of the fusion of BCG-ΔUT-infected phagosomes with lysosomes

The efficacy with which BCG-ΔUT-infected phagosomes fused with lysosomes in macrophages was examined using confocal microscopy. Lysosomes were stained with anti-LAMP1 mAb after treatment of THP-1 cells with FITC-labeled BCG-Tokyo or BCG-ΔUT for 24 h. The parental BCG colocalized with lysosomes less efficiently than BCG-ΔUT (data not shown). Therefore, BCG-ΔUT may at least partially enhance the ability to induce phagosomal maturation.

T-cell-stimulating activity of BCG-ΔUT

The activity of BCG-ΔUT to stimulate IFN-γ-producing CD4$^+$ T cells, when infected to macrophages, was assessed (Fig. 2). BCG-ΔUT-infected macrophages activated unseparated CD4$^+$ T cells to release IFN-γ substantially more efficiently than parent BCG-infected macrophages. Although BCG-ΔUT-infected macrophages also induced production of IL-2 from CD4$^+$ T cells (data not shown), the extent of IFN-γ (< 50 pg mL^{-1}) and IL-2 production was not as high as expected. Furthermore, BCG-ΔUT did not induce the activation of naïve CD4$^+$ T cells (data not shown). As the activation of T cells is largely influenced by the cytokine milieu, in which T cells and their stimulators

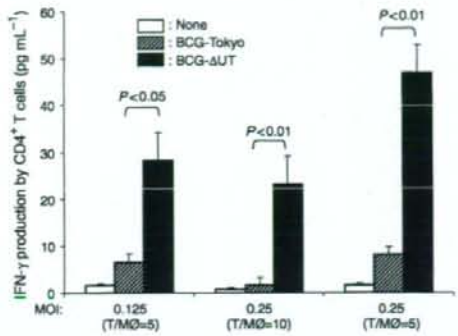

Fig. 2. Production of IFN-γ by CD4$^+$ T cells. Macrophages, differentiated by 5 days of culture with rM-CSF from monocytes, were infected with BCG-Tokyo (parental BCG) or BCG-ΔUT at the indicated MOI, and cultured for another 2 days in the presence of rM-CSF. These macrophages were used as a stimulator of autologous CD4$^+$ T cells (1×10^5 cells well^{-1}) at the indicated T-cell/macrophage ratio in a 4-day culture. A representative example of three separate experiments is shown. Assays were performed in triplicate and the results are expressed as the means ± SD. Titers were statistically compared using Student's *t*-test.

are present, we determined the level of cytokines produced from macrophages on stimulation with BCG-ΔUT. BCG-ΔUT produced significantly more cytokines, such as IL-10, GM-CSF, TNFα and IL-1β, than the parental BCG (data not shown). It has been reported that IL-10 inhibits the APC-mediated activation of T cells (Granelli-Piperno *et al.*, 2004) and GM-CSF regulates the function of macrophages (Makino *et al.*, 2007). To examine the role of IL-10 on T-cell activation, macrophages were infected with BCGs in the presence of a neutralizing mAb to IL-10 (Fig. 3a). The IFN-γ production by stimulated CD4$^+$ T cells was not influenced by the treatment of macrophages with control IgG; however, a significantly higher level of IFN-γ was produced on treatment with the neutralizing mAb to IL-10. The up-regulation by IL-10 mAb treatment was observed in both BCG-Tokyo and BCG-ΔUT in a similar fashion. Furthermore, the pretreatment of macrophages with exogenous GM-CSF also significantly upregulated the antigen-presenting function of macrophages, although the effect of GM-CSF was more pronounced in BCG-ΔUT-infected macrophages (Fig. 3b).

Next, we phenotypically assessed the effect of BCG-ΔUT on macrophages (Fig. 4a). BCG-ΔUT induced enhanced expression of both CD14 and CD40 on macrophages compared with BCG-Tokyo. Based on these results, we treated BCG-infected macrophages with CD40L to examine its role as a costimulator of macrophages (Fig. 4b). The CD40L treatment upregulated the T-cell activation by BCG-

© 2008 Federation of European Microbiological Societies
Published by Blackwell Publishing Ltd. All rights reserved

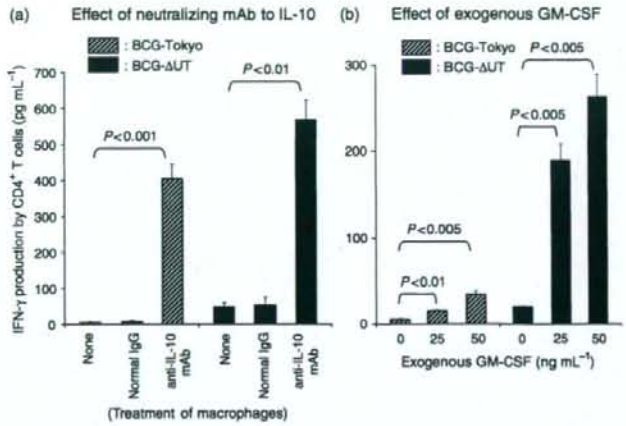

Fig. 3. Effect of IL-10 and GM-CSF on IFN-γ production. (a) Macrophages differentiated from monocytes by using rM-CSF were infected with either BCG-Tokyo or BCG-ΔUT at an MOI of 0.25 on day 5 of culture and cultured for another 2 days in the presence of rM-CSF. The BCG-infected macrophages were treated with neutralizing mAb to IL-10 or isotype-matched control IgG (10 μg mL^{-1}), and used as a stimulator of CD4$^+$ T cells, at a T-cell/macrophage ratio of 10 : 1, and cultured for another 4 days. The optimal concentration of mAb was determined in advance. (b) Macrophages obtained by 4 days of culture with rM-CSF were treated with the indicated dose of rGM-CSF. The macrophages pretreated with rGM-CSF were infected with BCG-Tokyo or BCG-ΔUT at an MOI of 0.25, cultured for another 2 days in the presence of rM-CSF used as a stimulator of CD4$^+$ T cells on day 8, at a T-cell/macrophage ratio of 10 : 1 (4 days of stimulation). A representative example of three separate experiments is shown. Assays were performed in triplicate and the results are expressed as the means ± SD. Titers were statistically compared using Student's *t*-test.

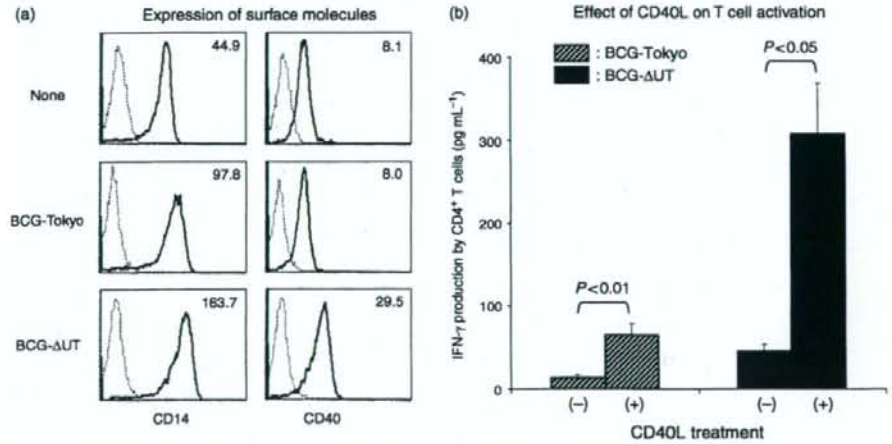

Fig. 4. (a) Expression of CD14 and CD40 molecules on macrophages. Macrophages produced by using rM-CSF were infected with BCGs at an MOI of 0.25, and cultured for another 2 days in the presence of rM-CSF. The macrophages on day 7 of culture were gated and analyzed. Dotted lines, isotype-matched control IgG; solid lines, the indicated test mAb. The number in the top right-hand corner of each panel represents the difference in mean fluorescence intensity between the control IgG and the test mAb. Representative results of three separate experiments are shown. (b) IFN-γ production by CD4$^+$ T cells stimulated with BCG-infected macrophages. Macrophages differentiated from monocytes using rM-CSF were infected with BCGs at an MOI of 0.25 on day 5 of culture, further treated with CD40L (1 μg mL^{-1}) on day 6, and used as a stimulator of CD4$^+$ T cells (T-cell/macrophage ratio of 10 : 1, 4 days of stimulation). A representative of three separate experiments is shown. Assays were performed in triplicate and the results are expressed as the means ± SD. Titers were statistically compared using Student's *t*-test.

© 2008 Federation of European Microbiological Societies
Published by Blackwell Publishing Ltd. All rights reserved

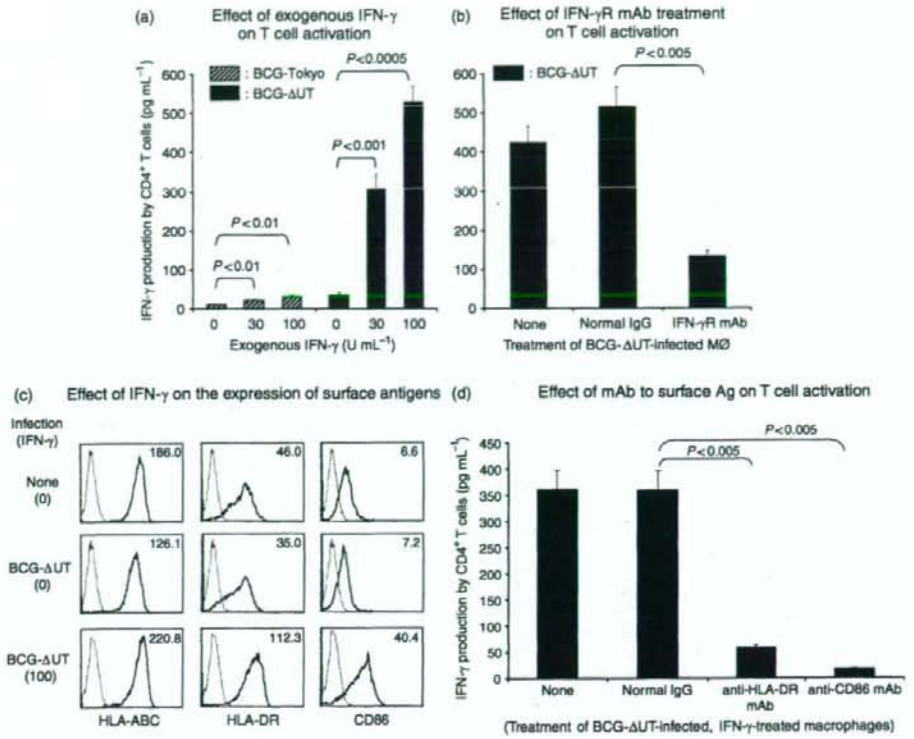

Fig. 5. (a) Effect of exogenous IFN-γ on CD4+ T-cell activation. Macrophages produced by 5 days of culture with rM-CSF from monocytes were infected with BCGs at an MOI of 0.25 and simultaneously treated with the indicated dose of exogenous IFN-γ. The macrophages were used as a stimulator of CD4+ T cells (T-cell/macrophage ratio of 10 : 1, 4 days of stimulation). A representative of three separate experiments is shown. Assays were performed in triplicate and the results are expressed as the means ± SD. Titers were statistically compared using Student's *t*-test. (b) Involvement of IFN-γ receptor in T-cell activation. Macrophages produced as in (a) were infected with BCG-ΔUT (MOI of 0.25), stimulated with exogenous IFN-γ (100 U mL^{-1}) in the presence of mAb to IFN-γ receptor α-chain (CD119) or isotype matched control IgG (10 μg mL^{-1}), and cultured for another 2 days in the presence of rM-CSF. The macrophages were used as a stimulator of CD4+ T cells (T-cell/macrophage ratio of 10 : 1, 4 days of stimulation). A representative of three separate experiments is shown. Assays were performed in triplicate and the results are expressed as the means ± SD. Titers were statistically compared using Student's *t*-test. (c) Surface expression of various molecules on BCG-ΔUT-infected, IFN-γ-treated macrophages. Macrophages produced as in (a) were infected with BCG-ΔUT (MOI of 0.25), stimulated with exogenous IFN-γ (100 U mL^{-1}) and cultured for another 2 days in the presence of rM-CSF. The macrophages on day 7 of culture were gated and analyzed. Dotted lines, isotype-matched control IgG; solid lines, the indicated test mAb. The number in the top right-hand corner of each panel represents the difference in mean fluorescence intensity between the control IgG and the test mAb. Representative results of three separate experiments are shown. (d) Involvement of surface antigens of BCG-ΔUT-infected, IFN-γ-stimulated macrophages in T-cell activation. Macrophages produced as in (a) were infected with BCG-ΔUT (MOI of 0.25), treated with exogenous IFN-γ (100 U mL^{-1}) and cultured for another 2 days in the presence of rM-CSF. These macrophages were cocultured with autologous CD4+ T cells at a T-cell/macrophage ratio of 10 : 1 in a 4-day culture in the presence of the indicated mAb (10 μg mL^{-1}). A representative of three separate experiments is shown. Assays were performed in triplicate and the results are expressed as the means ± SD. Titers were statistically compared using Student's *t*-test.

infected macrophages, but it more efficiently affected BCG-ΔUT-infected macrophages. Similarly, there was a significant difference between parent BCG and BCG-ΔUT in sensitivity to IFN-γ (Fig. 5a). However, other cytokines such as TNFα and IL-1β did not enhance the T-cell-stimulating activity of rBCG-infected macrophages. The IFN-γ treatment was effective against both BCG-Tokyo- and BCG-ΔUT-infected macrophages; however, more than a 10-fold increase in the production of IFN-γ from T cells was achieved only when BCG-ΔUT-infected macrophages

© 2008 Federation of European Microbiological Societies
Published by Blackwell Publishing Ltd. All rights reserved

were stimulated with exogenous IFN-γ. The optimal stimulation of T cells induced the production of more than 500 pg mL^{-1} IFN-γ. The exogenous IFN-γ seems to contribute directly to the enhancement of APC function, as the IFN-γ-mediated enhancement was cancelled out by the pretreatment of BCG-ΔUT-infected macrophages with mAb to IFN-γ receptor α-chain (Fig. 5b). Furthermore, IFN-γ significantly enhanced the expression of HLA-DR and CD86 on BCG-ΔUT-infected macrophages (Fig. 5c), while the phenotypic alteration of BCG-Tokyo-infected macrophages by IFN-γ was minimum (data not shown). When BCG-ΔUT-infected, IFN-γ-treated macrophages were treated with mAb to either HLA-DR or CD86 in advance of being cocultured with CD4$^+$ T cells, IFN-γ production by the T cells was significantly inhibited, while normal murine IgG treatment did not have any effect (Fig. 5d).

CD4$^+$ T-cell activation by BCG-ΔUT-infected DCs

As BCG-ΔUT significantly but less efficiently activated CD4$^+$ T cells through macrophages in the absence of costimulation, the potency of BCG-ΔUT-infected DCs as a T-cell activator was evaluated. Expression of surface molecules on DCs infected with either BCG-Tokyo or BCG-ΔUT was examined (Fig. 6a). Expression of HLA-ABC, HLA-DR, CD86 and CD83 was more significantly upregulated by the infection with BCG-ΔUT than with BCG-Tokyo. Higher levels of IL-12p70 and IL-1β were produced by BCG-ΔUT stimulation (Fig. 6b). Furthermore, we assessed whether BCG-ΔUT activated naïve and memory CD4$^+$ T cells through DCs by using various MOI titers and multiple T/DC ratios (Fig. 6c). IFN-γ levels were significantly higher following stimulation with BCG-ΔUT than with parent BCG in both naïve and memory CD4$^+$ T cells. Also, a higher level of CD40L was expressed on CD4$^+$ T cells after stimulation with BCG-ΔUT-infected DCs (data not shown). These results indicate that the infection of DCs with BCG-ΔUT alone was sufficient, as compared with macrophages which required costimulators to drive a strong T-cell response.

Memory T-cell production by BCG-ΔUT

Another important aspect of using BCG as a vaccine is the production of memory T cells *in vivo*. We examined the response of splenic T cells obtained from BCG-infected C57BL/6 mice to mycobacterial recall antigen (Fig. 7). We used BCC as a recall antigen. At 4 weeks following infection, splenic T cells from BCG-ΔUT-infected mice produced more IFN-γ than those from mice infected with BCG-Tokyo by responding to BCC. The lymphocyte population producing IFN-γ was found to be CD4$^+$ T cells by intracellular staining (data not shown). Furthermore, upon stimulation with MLM, which contains immunodominant antigens of *M. leprae*, CD4$^+$ T cells from BCG-ΔUT-infected mice produced significantly higher levels of IFN-γ than those from uninfected or BCG-Tokyo-infected mice (Fig. 7).

Discussion

To date, BCG is the only suitable vaccine against leprosy; however, its efficacy is quite limited. Overall efficacy in one meta-analysis was reported to be only 26% (Setia *et al.*, 2006). Several reasons might explain why BCG cannot block multiplication of *M. leprae* or inhibit the development of leprosy. The most important defect of BCG is that it is retained in phagosomes of macrophages, avoiding phagosomal acidification and hence interfering in the efficient fusion of BCG-containing phagosomes with lysosomes (Clements *et al.*, 1995; Reyrat *et al.*, 1995; Grode *et al.*, 2005). The lack of phagosome–lysosome fusion inhibits the trafficking of BCG-derived antigens through the major histocompatibility class (MHC) II pathway, which is enrolled for preferential stimulation of CD4$^+$ T cells, the most important cells involved in inhibition of *M. leprae* growth (Sendide *et al.*, 2004). Further, macrophages produce abundant amounts of IL-10 on infection with BCG, which, in turn, inhibits the activation of CD4$^+$ T cells (Mochida-Nishimura *et al.*, 2001; Granelli-Piperno *et al.*, 2004).

In the present study, we constructed a recombinant BCG (BCG-ΔUT) that lacks a *urease* gene through allelic exchange of chromosomal DNA. As urease is involved in the maintenance of intraphagosomal pH at neutral (Grode *et al.*, 2005) or slightly alkaline values (Sendide *et al.*, 2004), lack of this enzyme may contribute to the induction of phagosomal acidification (Sendide *et al.*, 2004), thereby promoting the fusion of BCG-containing phagosomes with lysosomes. The efficient colocalization of BCG-ΔUT with lysosome was observed, leading us to expect an efficient enhancement of T-cell activation by BCG-ΔUT-infected macrophages. Previously, rBCG deficient in urease C was produced by a similar system and found to be superior to parental BCG in producing acidic conditions (pH 4.5–5.5) in BCG-infected phagosomes in murine macrophages (Reyrat *et al.*, 1995; Grode *et al.*, 2005). However, it was not demonstrated whether the rBCG deficient in urease C promoted the MHC class II trafficking pathway and actually activated human CD4$^+$ T cells through APCs. The newly constructed BCG-ΔUT lacked urease activity and *in vitro* studies confirmed that it could not degrade urea to ammonia. When BCG-ΔUT was infected to macrophages, it activated human CD4$^+$ T cells more efficiently than the parental BCG. However, the amount of IFN-γ released from the T cells was not as high as expected (< 50 pg mL^{-1}). These results suggest that

© 2008 Federation of European Microbiological Societies
Published by Blackwell Publishing Ltd. All rights reserved

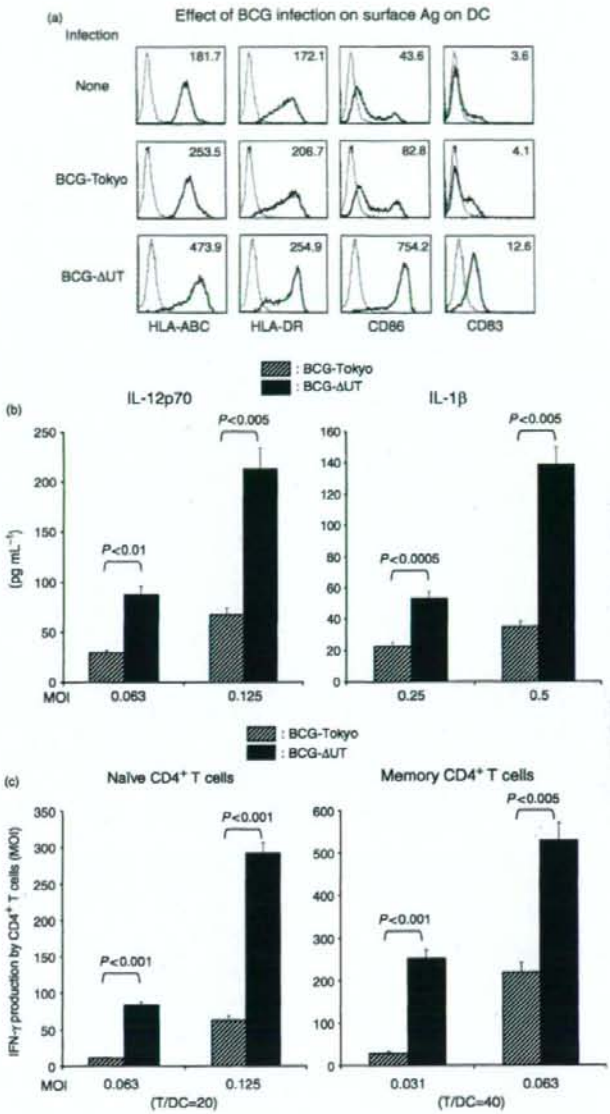

Fig. 6. (a) Expression of various molecules on BCG-infected DCs. Monocyte-derived immature DCs were infected with either BCG-Tokyo or BCG-ΔUT at an MOI of 0.25 and cultured for another 2 days in the presence of rGM-CSF and rIL-4. The DCs from day 5 were gated and analyzed. Dotted lines, isotype-matched control IgG; solid lines, the indicated test mAb. The number in the top right-hand corner of each panel represents the difference in mean fluorescence intensity between the control IgG and the test mAb. Representative results of three separate experiments are shown. (b) Cytokine production from DCs stimulated by BCG. Monocyte-derived DCs from 4 days of culture in the presence of rGM-CSF and rIL-4 were stimulated with the indicated dose of either BCG-Tokyo or BCG-ΔUT for 24 h. The concentration of the indicated cytokine was determined by the ELISA method. A representative of three separate experiments is shown. Assays were performed in triplicate and the results are expressed as the means ± SD. Titers were statistically compared using Student's *t*-test. (c) IFN-γ production by naïve CD4+ T cells and memory CD4+ T cells. DCs obtained from monocytes infected with either BCG-Tokyo or BCG-ΔUT were used as a stimulator of naïve and memory CD4+ T cells in a 4-day culture. A representative of three separate experiments is shown. Assays were performed in triplicate and the results are expressed as the means ± SD. Titers were statistically compared using Student's *t*-test.

improvement of intraphagosomal pH milieu for efficient phagosome–lysosome fusion was not sufficient for the induction of full T-cell activation as far as macrophages were concerned. Thus, we further searched for factors which might be helpful in inducing full activation of T cells. First, we examined the influence of endogenously produced IL-10, as abundant IL-10 was produced from macrophages by infection with BCG-ΔUT (data not shown). The neutralization of IL-10 from macrophages drastically enhanced T-cell activation (Fig. 3a). Furthermore, pretreatment of

© 2008 Federation of European Microbiological Societies
Published by Blackwell Publishing Ltd. All rights reserved

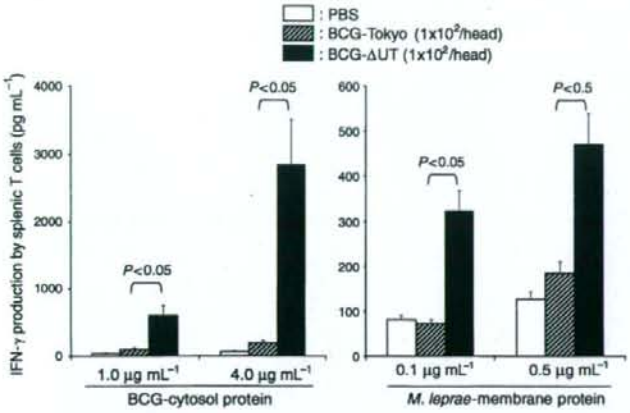

Fig. 7. IFN-γ production by splenic T cells obtained from C57BL/6 mice infected with BCG-Tokyo or BCG-ΔUT. Five-week-old C57BL/6 mice were infected with the indicated dose of BCG intradermally. Four weeks after the inoculation, splenocytes (2×10^5 cells well^{-1}) were stimulated with the indicated dose of either BCG-derived cytosol protein or *Mycobacterium leprae*-derived membrane protein for 4 days. Assays were performed in triplicate for each mouse, and the results for three mice per group are given, expressed as the means ± SD. Representative results for two separate experiments are shown. Titers were statistically compared using Student's *t*-test.

macrophages with GM-CSF, which is normally produced from activated $CD4^+$ T cells, monocytes and macrophages (data not shown), and inhibits IL-10 production (Makino *et al.*, 2007), was also quite efficient in enhancing the BCG-ΔUT-mediated T-cell activity. Therefore, the unexpectedly weak activation of $CD4^+$ T cells by BCG-ΔUT seemed to be at least partly due to the immunosuppressive effect of IL-10. Secondly, we focused on the costimulating factors capable of actively up-regulating the T-cell-stimulating function of macrophages, and found that both CD40L and IFN-γ were quite efficient. It was previously reported that both CD40L and IFN-γ were needed to costimulate macrophages infected with *M. leprae* (Makino *et al.*, 2007); however, in the present study, the sole treatment of BCG-ΔUT-infected macrophages with either CD40L or IFN-γ was enough to confer a sufficient effect (Figs 4 and 5). The high sensitivity of BCG-ΔUT-infected macrophages to CD40L may be due to the ability of rBCG to induce greater expression of CD40 (Fig. 4a). The exogenous IFN-γ may contribute to increased production of IFN-γ from T cells by activating macrophages, as it enhanced the surface expression of HLA-DR and CD86 on BCG-ΔUT-infected macrophages, which facilitated antigen-specific T-cell activation. As reported, *M. leprae* is less sensitive to IFN-γ (Makino *et al.*, 2007), and also parental BCG was found to be clearly less sensitive to IFN-γ than BCG-ΔUT. These results indicate that each mycobacterium may have differential sensitivity to IFN-γ (Verreck *et al.*, 2004). Although the molecular mechanism responsible for the difference in sensitivity remains unexplained, it is well known that IFN-γ facilitates the digestion of intracellular mycobacteria in macrophages, and thus the following speculation may be possible: in the present system, the alteration of the pH milieu of BCG-containing phagosomes caused by the depletion of urease activity may help to establish circumstances where cell activation as well as enhanced trafficking of mycobacterial antigens to the surface by the MHC class II pathway can be induced by IFN-γ treatment. The urease gene of pathogenic mycobacteria may be a good target for combination immunotherapy/chemotherapy as urease depletion downregulates the growth of mycobacteria (data not shown) and upregulates the immunoactivity of intracellular digestion of bacteria in host cells.

In contrast to macrophages, DCs were highly activated by the sole infection with BCG-ΔUT in terms of phenotype and cytokine production, and BCG-ΔUT-infected DCs efficiently activated both naïve and memory $CD4^+$ T cells in the absence of additional costimulation. The activated T cells produced abundant amounts of both IFN-γ (Fig. 5c) and GM-CSF, and induced CD40L expression (data not shown). Therefore, DCs can inherently provide the critical factors needed by BCG-ΔUT-infected macrophages. As BCG infects both macrophages and DCs *in vivo*, we evaluated the efficacy of BCG-ΔUT as a T-cell activator by using C57BL/6 mice. BCG-ΔUT was superior to BCG-Tokyo in the production of murine memory $CD4^+$ T cells, which can respond to BCG-derived recall antigen and also proteins derived from pathogenic *M. leprae*. Just 100 BCG-ΔUT bacilli were sufficient to produce such memory T cells. These findings indicate that BCG-ΔUT convincingly stimulated $CD4^+$ T cells *in vivo*. As the C57BL/6 strain is a T helper (Th)1 response-prone mouse, further study using Th2 response-prone mice would provide further insight into how memory T cells are generated by inoculation with BCG-ΔUT.

Taking our data together, BCG-ΔUT is more potent than the parental BCG in the activation of macrophages, DCs and $CD4^+$ T cells. The depletion of urease from BCG may be useful in upregulating the potency of BCG as an immunostimulator.

© 2008 Federation of European Microbiological Societies
Published by Blackwell Publishing Ltd. All rights reserved

Acknowledgements

We acknowledge the contribution of Ms N. Makino in the preparation of the manuscript. We thank Ms Y. Harada for her technical support and the Japanese Red Cross Society for kindly providing blood from healthy donors. We also thank Professor William R. Jacobs, Jr, Howard Hughes Medical Institute, for providing the plasmids, pYUB854 and phAE87. This work was supported in part by a Grant-in-Aid for Research on Emerging and Re-emerging Infectious Diseases from the Ministry of Health, Labour, and Welfare of Japan.

References

Andersen P & Doherty TM (2005) The success and failure of BCG-implications for a novel tuberculosis vaccine. *Nat Rev Microbiol* **3**: 656–662.

Bardarov S, Bardarov S Jr, Pavelka MS Jr, Sambandamurthy V, Larsen M, Tufariello J, Chan J, Hatfull G & Jacobs WR Jr (2002) Specialized transduction: an efficient method for generating marked and unmarked targeted gene disruptions in *Mycobacterium tuberculosis*, *M. bovis* BCG and *M. smegmatis*. *Microbiology* **148**: 3007–3017.

Charles C & Shepard MD (1960) The experimental disease that follows the injection of human leprosy bacilli into foot-pads of mice. *J Exp Med* **112**: 445–454.

Clements DL, Lee BY & Horwitz MA (1995) Purification, characterization, and genetic-analysis of *Mycobacterium tuberculosis* urease, a potentially critical determinant of host-pathogen interaction. *J Bacteriol* **177**: 5644–5652.

Dockrell HM, Young SK, Britton K *et al.* (1996) Induction of Th1 cytokine responses by mycobacterial antigens in leprosy. *Infect Immun* **64**: 4385–4389.

Dye C, Watt CJ, Bleed DM, Hosseini SM & Raviglione MC (2005) Evolution of tuberculosis control and prospects for reducing tuberculosis incidence, prevalence, and deaths globally. *JAMA* **293**: 2767–2775.

Granelli-Piperno A, Golebiowska A, Trumpfheller C, Siegal FP & Steinman RM (2004) HIV-1-infected monocyte-derived dendritic cells do not undergo maturation but can elicit IL-10 production and T cell regulation. *Proc Natl Acad Sci USA* **101**: 7669–7674.

Grode L, Seiler P, Baumann S *et al.* (2005) Increased vaccine efficacy against tuberculosis of recombinant *Mycobacterium bovis* bacille Calmette-Guérin mutants that secrete listeriolysin. *J Clin Investig* **115**: 2472–2479.

Hashimoto K, Maeda Y, Kimura H, Suzuki K, Masuda A, Matsuoka M & Makino M (2002) *Mycobacterium leprae* infection in monocyte-derived dendritic cells and its influence on antigen-presenting function. *Infect Immunity* **70**: 5167–5176.

Honerzu Bentrup K & Russell DG (2001) Mycobacterial persistence: adaptation to a changing environment [review]. *Trends Microbiol* **9**: 597–605.

Job CK (1989) Nerve damage in leprosy. *Int J Lepr Other Mycobact Dis* **57**: 532–539.

Kai M, Maeda Y, Maeda S, Fukutomi Y, Kobayashi K, Kashiwabara Y, Makino M, Abbasi MA, Khan MZ & Shah PA (2004) Active surveillance of leprosy contacts in country with low prevalence rate. *Int J Lepr Other Mycobact Dis* **72**: 50–53.

Kaufmann SHE (2005) Introduction. Rational vaccine development against tuberculosis: "those who don't remember the past are condemned to repeat it". *Microbes Infect* **7**: 897–898.

Kaufmann SHE (2006) Envisioning future strategies for vaccination against tuberculosis. *Nat Rev Immunol* **6**: 699–704.

Kaufmann SHE & McMichael AJ (2005) Annulling a dangerous liaison: vaccination strategies against AIDS and tuberculosis. *Nat Med* **11**: S33–S44.

Maeda S, Matsuoka M, Nakata N, Kai M, Maeda Y, Hashimoto K, Kimura H, Kobayashi K & Kashiwabara Y (2001) Multidrug resistant *Mycobacterium leprae* from patients with leprosy. *Antimicrob Agents Chemother* **45**: 3635–3639.

Maeda Y, Gidoh M, Ishii N, Mukai C & Makino M (2003) Assessment of cell mediated immunogenicity of *Mycobacterium leprae*-derived antigens. *Cell Immunol* **222**: 69–77.

Makino M & Baba M (1997) A cryopreservation method of human peripheral blood mononuclear cells for efficient production of dendritic cells. *Scand J Immunol* **45**: 618–622.

Makino M, Shimokubo S, Wakamatsu S, Izumo S & Baba M (1999) The role of human T-lymphotropic virus type I (HTLV-1)-infected dendritic cells in the development of HTLV-1-associated myelopathy/tropical spastic paraparesis. *J Virol* **73**: 4575–4581.

Makino M, Maeda Y, Fukutomi Y & Mukai T (2007) Contribution of GM-CSF on the enhancement of the T cell-stimulating activity of macrophages. *Microbes Infect* **9**: 70–77.

McDermott-Lancaster RD, Ito T, Kohsaka K, Guelpa-Lauras CC & Grosset JH (1987) Multiplication of *Mycobacterium leprae* in the nude mouse, and some applications of nude mice to experimental leprosy. *Int J Lepr Other Mycobact Dis* **55**: 889–895.

Miyamoto Y, Mukai T, Takeshita F, Nakata N, Maeda Y, Kai M & Makino M (2004) Aggregation of mycobacteria caused by disruption of fibronectin-attachment protein-encoding gene. *FEMS Microbiol Lett* **236**: 227–234.

Miyamoto Y, Mukai T, Nakata N, Maeda Y, Kai M, Naka T, Yano I & Makino M (2006) Identification and characterization of the genes involved in glycosylation pathways of mycobacterial glycopeptidolipid biosynthesis. *J Bacteriol* **188**: 86–95.

Mochida-Nishimura K, Akagawa KS & Rich EA (2001) Interleukin-10 contributes development of macrophage suppressor activities by macrophage colony-stimulating factor, but not by granulocyte-macrophage colony-stimulating factor. *Cell Immunol* **214**: 81–88.

Orme IM, Roberts AD, Griffin JP & Abrams JS (1993) Cytokine secretion by CD4 T lymphocytes acquired in response to *Mycobacterium tuberculosis* infection. *J Immunol* **151**: 518–525.

Reyrat JM, Berthet FX & Gicquel B (1995) The urease locus of *Mycobacterium tuberculosis* and its utilization for the

© 2008 Federation of European Microbiological Societies
Published by Blackwell Publishing Ltd. All rights reserved

demonstration of allelic exchange in *Mycobacterium bovis* bacillus Calmette-Guérin. *Proc Natl Acad Sci USA* **92**: 8768–8772.

Schaible UE, Sturgill-Koszycki S, Schlesinger PH & Russell DG (1998) Cytokine activation leads to acidification and increases maturation of *Mycobacterium avium*-containing phagosomes in murine macrophages. *J Immunol* **160**: 1290–1296.

Sendide K, Degmane AE, Reyrat JM, Talal A & Hmama Z (2004) *Mycobacterium bovis* BCG urease attenuates major histocompatibility complex class II trafficking to the macrophage cell surface. *Infect Immun* **72**: 4200–4209.

Setia MS, Steinmaus C, Ho CH & Rutherford GW (2006) The role of BCG in prevention of leprosy: a meta-analysis. *Lancet Infect Dis* **6**: 162–170.

Stoner GL (1979) Importance of the neural predilection of *Mycobacterium leprae* in leprosy. *Lancet* **2**: 994–996.

Verreck FA, de Boer T, Langenberg DM, Hoeve MA, Kramer M, Vaisberg E, Kastelein R, Kolk A, de Waal-Malefyt R & Ottenhoff TH (2004) Human IL-23-producing type 1 macrophages promote but IL-10-producing type 2 macrophages subvert immunity to (myco)bacteria. *Proc Natl Acad Sci USA* **101**: 4560–4565.

Wakamatsu S, Makino M, Tei C & Baba M (1999) Monocyte-driven activation-induced apoptotic cell death of human T-lymphotropic virus type I-infected T cells. *J Immunol* **163**: 3914–3919.

World Health Organization. (2006) *Fact Sheet No. 104*, Rev March, http://www.who.int/mediacentre/factsheets/fs104/en

© 2008 Federation of European Microbiological Societies
Published by Blackwell Publishing Ltd. All rights reserved

JOURNAL OF BACTERIOLOGY, May 2008, p. 3613–3621 Vol. 190, No. 10
0021-9193/08/$08.00+0 doi:10.1128/JB.01850-07
Copyright © 2008, American Society for Microbiology. All Rights Reserved.

Structural Analysis and Biosynthesis Gene Cluster of an Antigenic Glycopeptidolipid from *Mycobacterium intracellulare*▽†

Nagatoshi Fujiwara,[1]* Noboru Nakata,[2] Takashi Naka,[1,3] Ikuya Yano,[3] Matsumi Doe,[4] Delphi Chatterjee,[5] Michael McNeil,[5] Patrick J. Brennan,[5] Kazuo Kobayashi,[6] Masahiko Makino,[2] Sohkichi Matsumoto,[1] Hisashi Ogura,[7] and Shinji Maeda[8]

Department of Host Defense[1] and Virology,[7] Osaka City University Graduate School of Medicine, Osaka 545-8585, Japan; Department of Microbiology, Leprosy Research Center, National Institute of Infectious Diseases, Tokyo 189-0002, Japan[2]; Japan BCG Laboratory, Tokyo 204-0022, Japan[3]; Department of Chemistry, Graduate School of Science, Osaka City University, Osaka 558-8585, Japan[4]; Department of Microbiology, Immunology and Pathology, Colorado State University, Colorado 80523[5]; Department of Immunology, National Institute of Infectious Diseases, Tokyo 162-8640, Japan[6]; and Molecular Epidemiology Division, Mycobacterium Reference Center, The Research Institute of Tuberculosis, Japan Anti-Tuberculosis Association, Tokyo 204-8533, Japan[8]

Received 24 November 2007/Accepted 1 March 2008

***Mycobacterium avium-Mycobacterium intracellulare* complex (MAC) is the most common isolate of nontuberculous mycobacteria and causes pulmonary and extrapulmonary diseases. MAC species can be grouped into 31 serotypes by the epitopic oligosaccharide structure of the species-specific glycopeptidolipid (GPL) antigen. The GPL consists of a serotype-common fatty acyl peptide core with 3,4-di-*O*-methyl-rhamnose at the terminal alaninol and a 6-deoxy-talose at the *allo*-threonine and serotype-specific oligosaccharides extending from the 6-deoxy-talose. Although the complete structures of 15 serotype-specific GPLs have been defined, the serotype 16-specific GPL structure has not yet been elucidated. In this study, the chemical structure of the serotype 16 GPL derived from *M. intracellulare* was determined by using chromatography, mass spectrometry, and nuclear magnetic resonance analyses. The result indicates that the terminal carbohydrate epitope of the oligosaccharide is a novel *N*-acyl-dideoxy-hexose. By the combined linkage analysis, the oligosaccharide structure of serotype 16 GPL was determined to be 3-2′-methyl-3′-hydroxy-4′-methoxy-pentanoyl-amido-3,6-dideoxy-β-hexose-(1→3)-4-*O*-methyl-α-L-rhamnose-(1→3)-α-L-rhamnose-(1→3)-α-L-rhamnose-(1→2)-6-deoxy-α-L-talose. Next, the 22.9-kb serotype 16-specific gene cluster involved in the glycosylation of oligosaccharide was isolated and sequenced. The cluster contained 17 open reading frames (ORFs). Based on the similarity of the deduced amino acid sequences, it was assumed that the ORF functions include encoding three glycosyltransferases, an acyltransferase, an aminotransferase, and a methyltransferase. An *M. avium* serotype 1 strain was transformed with cosmid clone no. 253 containing *gtfB-drrC* of *M. intracellulare* serotype 16, and the transformant produced serotype 16 GPL. Together, the ORFs of this serotype 16-specific gene cluster are responsible for the biosynthesis of serotype 16 GPL.**

Mycobacterial diseases, such as tuberculosis and infection due to nontuberculous mycobacteria (NTM), are still among the most serious infectious diseases in the world. The incidence is increasing because of the spread of drug-resistant mycobacteria and the human immunodeficiency virus (HIV) infection/AIDS epidemic (16, 17, 30). *Mycobacterium avium-Mycobacterium intracellulare* complex (MAC) is the most common among isolates of NTM and is distributed ubiquitously in the environment. MAC causes pulmonary and extrapulmonary diseases in both immunocompromised and immunocompetent hosts. It affects primarily patients with advanced HIV infection. MAC includes at least two mycobacterial species, *M. avium* and *M. intracellulare*, that cannot be differentiated on the basis of traditional physical and biochemical tests (1, 41).

The cell envelope of mycobacteria is a complex and unusual structure. The key feature of this structure is an extraordinarily high lipid concentration (6, 10). To better understand the pathogenesis of MAC infection, it is necessary to elucidate the molecular structure and biochemical features of the lipid components. Among MAC lipids, the glycopeptidolipid (GPL) is of particular importance, because it shows not only serotype-specific antigenicity but also immunomodulatory activities in the host immune responses (2, 9, 23). Structurally, GPLs are composed of two parts, a tetrapeptide-amino alcohol core and a variable oligosaccharide (OSE). C_{26}-C_{34} fatty acyl-D-phenylalanine-D-*allo*-threonine-D-alanine-L-alaninol (D-Phe-D-*allo*-Thr-D-Ala-L-alaninol) is further linked with 6-deoxy talose (6-d-Tal) and 3,4-di-*O*-methyl rhamnose (3,4-di-*O*-Me-Rha) at D-*allo*-Thr and the terminal L-alaninol, respectively. This type of core GPL is found in all subspecies of MAC, shows a common antigenicity, and is further glycosylated at 6-d-Tal to form a serotype-specific OSE.

At present, 31 distinct serotype-specific GPLs have been identified serologically and chromatographically (9). Although the standard technique for differentiation of MAC subspecies

* Corresponding author. Mailing address: Department of Host Defense, Osaka City University Graduate School of Medicine, 1-4-3 Asahi-machi, Abeno-ku, Osaka 545-8585, Japan. Phone: 81 6 6645 3746. Fax: 81 6 6645 3747. E-mail: fujiwara@med.osaka-cu.ac.jp.

† Supplemental material for this article may be found at http://jb.asm.org/.

▽ Published ahead of print on 7 March 2008.

has been serotyping based on the OSE residue of its GPL, the complete structures of only 15 GPLs have been defined. In addition to the chemical structures of various GPLs, genes encoding the glycosylation pathways in the biosynthesis of GPL have been identified and characterized (12, 21, 31). Epidemiological studies have shown that MAC serotypes 4 and 8 are the most frequently isolated from patients, and MAC serotype 16 is one of the next most common groups (32, 40). It has been suggested that the serotypes of MAC isolates participate in their virulence (29), and thus, understanding of the structure-pathogenicity relationship of GPLs is necessary. In the present study, we demonstrate the complete OSE structure of the GPL derived from serotype 16 MAC (*M. intracellulare*), which has a unique terminal-acylated-amido sugar, and we characterized the serotype 16 GPL-specific gene cluster involved in the glycosylation of carbohydrates.

MATERIALS AND METHODS

Bacterial strains and preparation of GPL. *M. intracellulare* serotype 16 strain ATCC 13950^T (NF 115) was purchased from the American Type Culture Collection (Manassas, VA). Three clinical isolates of *M. intracellulare* serotype 16 (NF 116 and 117) and *M. avium* serotype 1 (NF 113) were maintained in The Research Institute of Tuberculosis, Japan Anti-Tuberculosis Association. The preparation of GPL was performed as described previously (18, 24, 26). Briefly, each strain of *M. intracellulare* serotype 16 was grown in Middlebrook 7H9 broth (Difco Laboratories, Detroit, MI) with 0.5% glycerol and 10% Middlebrook oleic acid-albumin-dextrose-catalase enrichment (Difco) at 37°C for 2 to 3 weeks. The heat-killed bacteria were sonicated, and crude lipids were extracted with chloroform-methanol (2:1, vol/vol). The extracted lipids were dried and hydrolyzed with 0.2 N sodium hydroxide in methanol at 37°C for 2 h. After neutralization with 6 N hydrochloric acid, alkaline-stable lipids were partitioned by a two-layer system of chloroform-methanol (2:1, vol/vol) and water. The organic phase was recovered, evaporated, and precipitated with acetone to remove any acetone-insoluble components containing phospholipids and glycolipids. The supernatant was collected by centrifugation, dried, and then treated with a Sep-Pak silica cartridge (Waters Corporation, Milford, MA) with washing (chloroform-methanol, 95:5, vol/vol) and elution (chloroform-methanol, 1:1, vol/vol) for partial purification. GPL was completely purified by preparative thin-layer chromatography (TLC) of Silica Gel G (20 by 20 cm, 250 μm; Uniplate; Analtech, Inc., Newark, DE). The TLC plate was repeatedly developed with chloroform-methanol-water (65:25:4 and 60:16:2, vol/vol/vol) until a single spot was obtained. After exposure of the TLC plate to iodine vapor, the GPL band was marked, and then, the silica gels were scraped off and the GPL was eluted with chloroform-methanol (2:1, vol/vol).

Preparation of OSE moiety. β elimination of GPL was performed with alkaline borohydride, and the OSE elongated from D-*allo*-Thr was released as described previously (18, 24). Briefly, the GPL was dissolved in ethanol, and an equal volume of 10 mg/ml sodium borohydride or borodeuteride in 0.5 N sodium hydroxide was added and then stirred at 60°C for 16 h. The reaction mixture was decationized with Dowex 50W-X8 beads (Dow Chemical Company, Midland, MI), collected, and evaporated under nitrogen to remove boric acid. The dried residue was partitioned in two layers of chloroform-methanol (2:1, vol/vol) and water. The upper aqueous phase was recovered and evaporated. In these processes, the serotype 16-specific OSE was purified as an oligoglycosyl alditol.

MALDI-TOF and MALDI-TOF/TOF MS analyses. The molecular species of the intact GPL was detected by matrix-assisted laser desorption ionization–time of flight mass spectrometry (MALDI-TOF MS) with an Ultraflex II (Bruker Daltonics, Billerica, MA). The GPL was dissolved in chloroform-methanol (2:1, vol/vol) at a concentration of 1 mg/ml, and 1 μl was applied directly to the sample plate, and then 1 μl of 10 mg/ml 2,5-dihydroxybenzoic acid in chloroform-methanol (1:1, vol/vol) was added as a matrix. The intact GPL was analyzed in the reflectron mode with an accelerating voltage operating in a positive mode of 20 kV (5). Then the fragment pattern of the OSE was analyzed with MALDI-TOF/TOF MS. The OSE was dissolved in ethanol-water (3:7, vol/vol), and the matrix was 10 mg/ml 2,5-dihydroxybenzoic acid in ethanol-water (3:7, vol/vol). The OSE and the matrix were applied to the sample plate according to the method for intact GPL and analyzed in the lift-lift mode.

GC and GC-MS analyses of carbohydrates and *N*-acylated short-chain fatty acid. To determine the glycosyl composition and linkage position, gas chromatography (GC) and GC-MS analyses of partially methylated alditol acetate derivatives were performed. Perdeuteromethylation was conducted by the modified procedure of Hakomori as described previously (18, 20). Briefly, the dried OSE was dissolved with a mixture of dimethyl sulfoxide and sodium hydroxide, and deuteromethyl iodide was added. The reaction mixture was stirred at room temperature for 15 min and then water and chloroform were added. The chloroform-containing perdeuteromethylated OSE layer was collected, washed with water two times, and then completely evaporated. Partially deuteromethylated alditol acetates were prepared from perdeuteromethylated OSE by hydrolysis with 2 N trifluoroacetic acid at 120°C for 2 h, reduction with 10 mg/ml sodium borodeuteride at 25°C for 2 h, and acetylation with acetic anhydride at 100°C for 1 h (8, 18, 25). To identify amino-linked fatty acids, acidic methanolysis of serotype 16 GPL was performed with 1.25 M hydrogen chloride in methanol (Sigma-Aldrich, St. Louis, MO) at 100°C for 90 min, and the fatty acid methyl esters were extracted with *n*-hexane under the cooled ice. GC was performed using a 5890 series II gas chromatograph (Hewlett Packard, Avondale, PA) equipped with a fused SPB-1 capillary column (30 m, 0.25-mm inner diameter; Supelco Inc., Bellefonte, PA). Helium was used for electron impact (EI)-MS and isobutane for chemical ionization (CI)-MS as a carrier gas. A JMS SX102A double-focusing mass spectrometer (JEOL, Tokyo, Japan) was connected to the gas chromatograph as a mass detector. The molecular separator and the ion source energy were 70 eV for EI and 30 eV for CI, and the accelerating voltage was 8 kV. The D and L configurations of Rha residues were determined by comparative GC-MS analysis of trimethylsilylated (*S*)-(+)-sec-butyl glycosides and (*R*)-(−)-sec-butyl glycosides prepared from an authentic standard L-Rha (19).

NMR analysis of GPL. The GPL was dissolved in chloroform-d ($CDCl_3$)-methanol-d_4 (CD_3OD) (2:1, vol/vol). To define the anomeric configurations of each glycosyl residue, ^1H and ^{13}C nuclear magnetic resonance (NMR) was employed. Both homonuclear correlation spectrometry (COSY) and ^1H-detected [^1H, ^{13}C] heteronuclear multiple-quantum correlation (HMQC) were recorded with a Bruker Avance-600 (Bruker BioSpin Corp., Billerica, MA), as described previously (9, 18, 24, 34).

Construction of *M. intracellulare* serotype 16 cosmid library. A cosmid library of *M. intracellulare* serotype 16 strain ATCC 13950^T was constructed as described previously (18). Bacterial cells were disrupted mechanically, and genomic DNA was extracted with phenol-chloroform and then precipitated with ethanol. Genomic DNA randomly sheared into 30- to 50-kb fragments in the extraction process was fractionated and electroeluted from agarose gels using a Takara Recochip (Takara, Kyoto, Japan). These DNA fragments were rendered blunt ended using T4 DNA polymerase and deoxynucleoside triphosphates and then were ligated to dephosphorylated arms of pYUB412 (XbaI-EcoRV and EcoRV-XbaI), which were the kind gifts of William R. Jacobs, Jr. (Department of Microbiology and Immunology, Albert Einstein College of Medicine, Bronx, NY). The cosmid vector pYUB412 is an *Escherichia coli-Mycobacterium* shuttle vector with the *int-attP* sequence for integration into a mycobacterial chromosome, *oriE* for replication in *E. coli*, a hygromycin resistance gene, and an ampicillin resistance gene. After in vitro packaging using Gigapack III Gold extracts (Stratagene, La Jolla, CA), recombinant cosmids were introduced into *E. coli* STBL2 [F$^-$ *mcrA* Δ(*mcrBC-hsdRMS-mrr*) *recA1 endA1 lon gyrA96 thi supE44 relA1* λ Δ(*lac-proAB*)] and stored at −80°C in 50% glycerol.

Isolation of cosmid clones carrying biosynthesis gene cluster of serotype 16 GPL and sequence analysis. Isolation of DNA from *E. coli* transductants was performed as described by Supply et al., with modifications (39). The colonies were picked, transferred to a 1.5-ml tube containing 50 μl of water, and then heated at 98°C for 5 min. After centrifugation at 14,000 rpm for 5 min, the supernatant was used as the PCR template. PCR was used to isolate cosmid clones carrying the rhamnosyltransferase (*rtfA*) gene with primers rtfA-F (5′-TTTGGAGCGACGAGTTCATC-3′) and rtfA-R (5′-GTGTAGTTGACCACG CCGAC-3′). *rtfA* encodes an enzyme responsible for the transfer of Rha to 6-d-Tal in OSE (14, 31). The insert of cosmid clone no. 253 was sequenced using a BigDye Terminator, version 3.1, cycle sequencing kit (Applied Biosystems, Foster City, CA) and an ABI Prism 310 gene analyzer (Applied Biosystems). The putative function of each open reading frame (ORF) was identified by similarity searches between the deduced amino acid sequences and known proteins using BLAST (http://www.ncbi.nlm.nih.gov/BLAST/) and FramePlot (http://www.nih.go.jp/~jun/cgi-bin/frameplot.pl) with the DNASIS computer program (Hitachi Software Engineering, Yokohama, Japan).

Transformation of *M. avium* serotype 1 strain with cosmid clone no. 253. An *M. avium* serotype 1 strain (NF113) was transformed with pYUB412-cosmid clone no. 253 by electroporation, and hygromycin-resistant colonies were iso-

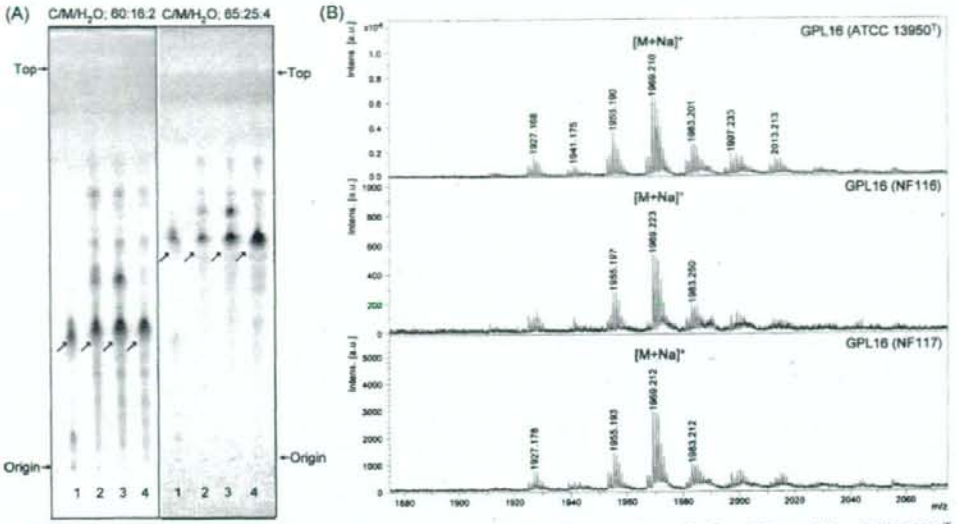

FIG. 1. TLC patterns and MALDI-TOF MS spectra of serotype 16 GPL. (A) Serotype 16 GPL purified from *M. intracellulare* ATCC 13950^T (NF 115) and the alkaline-stable lipids derived from ATCC 13950^T and two clinical isolates (NF 116 and 117) from left to right were developed on TLC plates with solvent systems of chloroform-methanol-water (65:25:4 and 60:16:2, vol/vol/vol). (B) The MALDI-TOF MS spectra were acquired using 10 mg/ml 2,5-dihydroxybenzoic acid in chloroform-methanol (1:1, vol/vol) as a matrix, and the molecularly related ions were detected as $[M+Na]^+$ in positive mode. Intens., intensity; a.u., absorbance units.

lated. Alkaline-stable lipids were prepared, and productive GPLs were examined by TLC and MALDI-TOF MS analyses.

Nucleotide sequence accession number. The nucleotide sequence reported here has been deposited in the NCBI GenBank database under accession no. AB355138.

RESULTS

Purification and molecular weight of intact GPL. Serotype 16 GPL from *M. intracellulare* ATCC 13950^T (NF 115) was detected as a spot by TLC, and the R_f values were 0.35 and 0.56 when developed with chloroform-methanol-water (60:16:2 and 65:25:4, vol/vol/vol, respectively). Two clinical isolates of *M. intracellulare*, NF 116 and 117, had serotype 16 GPLs that showed the same R_f values as the serotype 16 GPL derived from strain ATCC 13950^T. The serotype 16 GPL of *M. intracellulare* strain ATCC 13950^T was purified repeatedly by TLC and was shown as a single spot by TLC (Fig. 1A). The MALDI-TOF MS spectra of each serotype 16 GPL showed *m/z* 1969 for $[M+Na]^+$ as the main molecularly related ion in positive mode, with the homologous ions differing by 14 mass units at 1,955 and 1,983 (Fig. 1B). As a result, the main molecular weight of serotype 16 GPL was 1,946, which implied that it has a novel carbohydrate chain elongated from D-*allo*-Thr.

Carbohydrate composition of serotype 16 OSE. To determine the glycosyl compositions of serotype 16 OSE, alditol acetate derivatives of the serotype 16 GPL were analyzed by GC and GC-MS. The structurally defined serotype 4 GPL was used as a reference standard (9, 35). Comparison of the retention time and GC mass spectra (Fig. 2) with the alditol acetate derivatives of the serotype 16 GPL showed the presence of 3,4-di-*O*-Me-Rha, 4-*O*-Me-Rha, Rha, 6-d-Tal, and an unknown sugar residue (X1) in a ratio of approximately 1:1:2:1:1. The alditol acetate of X1 was eluted at a retention time of 29.3 min, greater than that of glucitol acetate on the SPB-1 column. The CI-MS spectrum of X1 was $[M+H]^+$ at *m/z* 520 as a parent ion and *m/z* 460 as a loss of 60 (acetate). The fragment ions of X1 sugar showed characteristic patterns in EI-MS. *m/z* 360 indicated the cleavage of C-3 and C-4, and *m/z* 300, 240, and 180 were fragmented with a loss of 60 (acetate). Similarly, *m/z* 374 indicated the cleavage of C-2 and C-3, and *m/z* 314 and 254 were fragmented with a loss of 60 (Fig. 3A and B). These results indicated that X1 was 3,6-dideoxy hexose (Hex). The odd molecular weight of X1, 519, and *m/z* 187, 127, and 59 implied the presence of one amido group esterified with a short-chain fatty acid, possibly. After methanolysis of serotype 16 GPL, the resultant fatty acid methyl esters were extracted carefully and analyzed by GC-MS. The EI-MS spectrum of a short-chain fatty acid methyl ester showed mass ions at *m/z* 176 ($[M]^+$), 145 ($[M-31]^+$), 117 ($[M-59]^+$), 99, 88, 85, and 59 (Fig. 3C) (33, 37). Taking the results together, X1 was structurally determined to be 3-2'-methyl-3'-hydroxy-4'-methoxy-pentanoyl-amido-3,6-dideoxy-Hex.

Glycosyl linkage and sequence of serotype 16 OSE. To determine the glycosyl linkage and sequence of the OSE, GC-MS of perdeuteromethylated alditol acetates and MALDI-TOF/TOF MS of the oligoglycosyl alditol from serotype 16 OSE

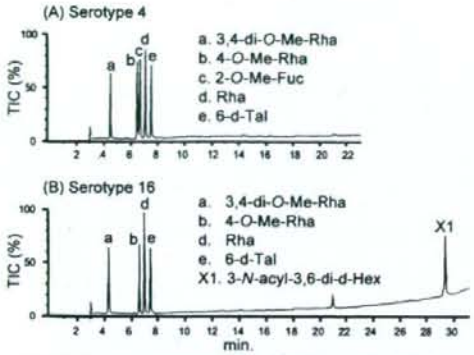

FIG. 2. Gas chromatograms of the alditol acetate derivatives from serotype 4 (A) and serotype 16 (B) GPLs. Total ion chromatograms (TIC) are shown. GC was performed on an SPB-1-fused silica column with a temperature program of 160°C for 2 min, followed by an increase of 4°C/min to 220°C, and holding at 220°C for 15 min. Comparison to the GC spectrum of serotype 4 GPL shows that serotype 16 GPL is composed of 3,4-di-*O*-Me-Rha, 4-*O*-Me-Rha, Rha, 6-d-Tal, and an unknown X1 sugar residue.

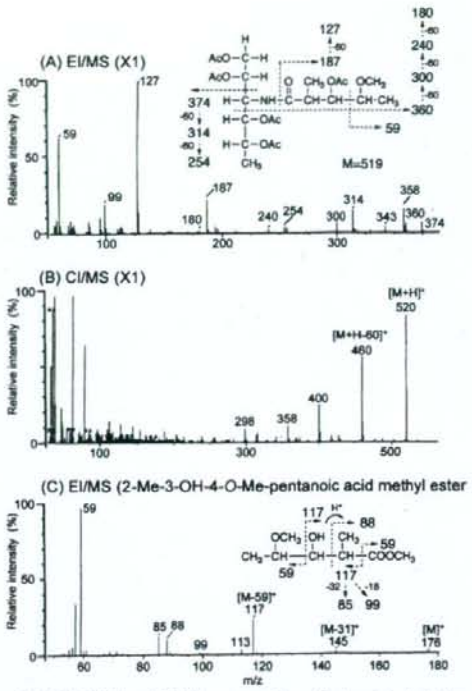

FIG. 3. EI-MS and CI-MS spectra of the alditol acetate derivative from X1 (A and B) and *N*-acylated-short-chain fatty acid methyl ester (C). The pattern of prominent fragment ions is illustrated. The CG column and condition were described in the legend for Fig. 2.

were performed. As shown in Fig. 4, the GC-MS spectra of perdeuteromethylated alditol acetates were assigned four major peaks, 1,3,4,5-tetra-*O*-deuteromethyl-2-*O*-acetyl-6-deoxytalitol (*m/z* 109, 132, 154, 167, and 214); 2,4-di-*O*-deuteromethyl-1,3,5-tri-*O*-acetyl-rhamnitol (*m/z* 121, 134, 205, 240, and 253); 2-*O*-deuteromethyl-4-*O*-methyl-1,3,5-tri-*O*-acetyl-rhamnitol (*m/z* 121, 131, 202, and 237); and 2,4-di-*O*-deuteromethyl-1,5-di-*O*-acetyl-3-2′-methyl-3′-*O*-deuteromethyl-4′methoxy-pentanoyl-deuteromethylamido-3,6-dideoxy-hexitol (*m/z* 121, 134, and 341). These results revealed that the 6-d-Tal residue was linked at C-2; Rha and 4-*O*-Me-Rha were linked at C-1 and C-3; and the nonreducing terminus, 3-2′-methyl-3′-hydroxy-4′-methoxy-pentanoyl-amido-3,6-dideoxy-Hex, was C-1 linked. The MALDI-TOF/TOF MS spectrum of the oligoglycosyl alditol from serotype 16 OSE afforded the expected molecular ions $[M+Na]^+$ at *m/z* 931, together with the characteristic mass increments in the series of glycosyloxonium ions formed on fragmentation at *m/z* 312, 472, 618, and 764 from the terminal sugar *N*-acyl-Hex to 6-d-Tal and at *m/z* 336, 482, and 642 from 6-d-Tal to *N*-acyl-Hex (Fig. 5). Rha residues were determined to be in the L absolute configuration by comparative GC-MS analyses of trimethylsilylated (*S*)-(+)-sec-butyl glycosides and (*R*)-(−)-sec-butylglycosides (see Fig. S1 in the supplemental material). Taken together, these results established the sequence and linkage arrangement 3-2′-methyl-3′-hydroxy-4′-methoxy-pentanoyl-amido-3,6-dideoxy-Hex-(1→3)-4-*O*-Me-Rha-(1→3)-L-Rha-(1→3)-L-Rha-(1→2)-6-d-Tal, exclusively.

NMR analysis of serotype 16 OSE. The ^{1}H NMR and ^{1}H-^{1}H COSY analyses of the serotype 16 GPL revealed six distinct anomeric protons with corresponding H1-H2 cross peaks in the low field region at δ4.93, 4.92, 4.92, 4.84, 4.65 ($J_{1\text{-}2}$ = 2 to 3 Hz, indicative of α-anomers) and 4.51 (a doublet, $J_{1\text{-}2}$ = 7.7 Hz, indicative of a β-hexosyl unit). When further analyzed by ^{1}H-detected [^{1}H, ^{13}C] two-dimensional HMQC, the anomeric protons resonating at δ4.93, 4.92, 4.92, 4.84, 4.65, and 4.51 have C-1s resonating at δ101.57, 95.73, 101.40, 102.56, 100.97, and 103.36, respectively (for a summary, see Table S1 in the supplemental material). The J_{CH} values for each of these protons were calculated to be 171, 170, 171, 170, 169, and 161 Hz by measurement of the inverse-detection nondecoupled two-dimensional HMQC (Fig. 6). These results established that the terminal amido-Hex was a β configuration and the others were α-anomers.

Cloning and sequence of serotype 16 GPL biosynthesis cluster. To isolate the serotype 16 GPL biosynthesis cluster, the genomic cosmid library of *M. intracellulare* serotype 16 strain ATCC 13950^T was constructed. Primers were designed to amplify the region corresponding to the *rtfA* gene. More than 300 cosmid clones were tested using colony PCR with *rtfA* primers, and the positive clones no. 51 and 253 were isolated from the *E. coli* transductants. PCR analysis revealed that clone no. 253 contained a *drrC* gene but that clone no. 51 did not. Thus, we used clone no. 253 for subsequent sequence analysis for the *gtfB-drrC* region. The 22.9-kb region of *M. intracellulare* sero-

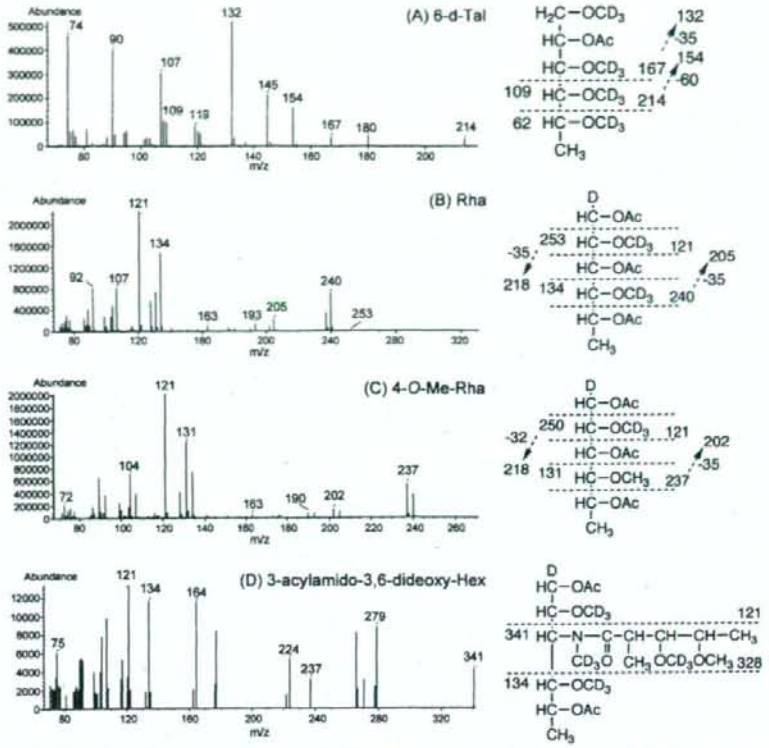

FIG. 4. GC-MS spectra of individual perdeuteromethylated alditol acetate derivatives from serotype 16 OSE. The formation of prominent fragment ions is illustrated; fragments were assigned to 1,3,4,5-tetra-*O*-deuteromethyl-2-*O*-acetyl-6-deoxy-talitol (A), 2,4-di-*O*-deuteromethyl-1,3,5-tri-*O*-acetyl-rhamnitol (B), 2-*O*-deuteromethyl-4-*O*-methyl-1,3,5-tri-*O*-acetyl-rhamnitol (C), and 2,4-di-*O*-deuteromethyl-1,5-di-*O*-acetyl-3-2'-methyl-3'-*O*-deuteromethyl-4'-methoxy-pentanoyl-deuteromethylamido-3,6-dideoxy-hexitol (D).

type 16 ATCC 13950^T was deposited in the NCBI GenBank database (accession no. AB355138). The similarity to protein sequences of each ORF is summarized in Table 1, and the genetic map for the serotype 16 GPL biosynthetic cluster was compared with those of serotype 2, 4, and 7 GPLs (Fig. 7). The *gtfB* and *drrC* genes of *M. intracellulare* serotype 16 ATCC 13950^T had 99.8% and 83.7% DNA identities with those of *M. intracellulare* serotype 7 ATCC 35847, respectively. In the DNA region between *gtfB* and *drrC* (20.8 kb), 17 ORFs were observed. Four ORFs (ORF 1, 2, 16, and 17) were homologous to those found in the same region of serotype 7-specific DNA, and the others were unique to the serotype 16 strain. No insertion of insertion elements or transposons was detected in this region. The nucleotide sequences of the ORF 1 and ORF 2 in serotype 16 strain ATCC 13950^T were homologous to those of ORF 1 and ORF 8 in serotype 7, respectively, suggesting that these two ORFs have the same function. The similarity of the deduced amino acid sequences suggested the possibility that the functions of ORF 3 and ORF 6 are to encode methyltransferase and aminotransferase, respectively. The deduced amino acid sequences of ORF 4 and ORF 5 showed significant similarities to the WxcM protein, the function of which is not clear. Interestingly, the deduced amino acid sequences of ORF 16 and ORF 17 of serotype 16 were homologous to ORF 9 of serotype 7. ORFs 1, 16, and 17 have considerable homology to glycosyltransferases. Nine ORFs, which are possibly involved in fatty acid synthesis, were detected between ORF 7 and ORF 15. It is notable that ORF 13 had a chimeric structure. The N-terminal half of ORF 13 showed similarity to phosphate butyryl/acetyl transferases, but the C-terminal half showed similarity to short-chain reductase/dehydrogenases. These results suggest that this region of DNA is responsible for the biosynthesis of the serotype 16-specific GPL.

Expression of cosmid clone no. 253 in *M. avium* serotype 1 strain. The OSE of serotype 1 GPL was composed of α-L-Rha-

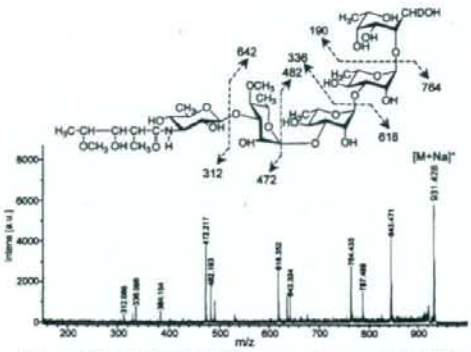

FIG. 5. MALDI-TOF/TOF MS spectrum of serotype 16 OSE. The formation of a characteristic increment in fragment ions is illustrated. The matrix was 10 mg/ml 2,5-dihydroxybenzoic acid in ethanol-water (3:7, vol/vol), and it was performed in the lift-lift mode. Intens., intensity; a.u., absorbance units.

(1→2)-6-d-L-Tal (9). The *M. avium* serotype 1 strain (NF113) was transformed with cosmid clone no. 253 containing a serotype 16-specific gene cluster and produced a new GPL with a different R_f value by TLC compared to serotype 1 GPL (Fig. 8A). The R_f value of the new GPL was identical to that of the serotype 16 GPL. The molecular weight of intact GPL, the fragment pattern of its OSE, and the GC pattern of the alditol acetate derivatives were completely equivalent to those of the serotype 16 GPL (see Fig. S2 in the supplemental material). As a result, the transformant of the serotype 1 strain expressed the cosmid clone no. 253 gene cluster and produced the serotype 16 GPL.

DISCUSSION

MAC species have serotype-specific GPLs that are characteristic components of the outer layer of the cell wall (6, 9). In addition to their serological differentiation, the chemical structures of 15 serotype-specific GPLs derived from the predominant clinical isolates have been analyzed; however, those of other GPLs remain unclear. The present study demonstrates the chemical structure of the serotype 16 GPL derived from *M. intracellulare*. We determined the glycosyl composition, linkage positions, and anomeric and ring configurations of the glycosyl residues of the serotype 16 GPL, and its OSE was defined as 3-2′-methyl-3′-hydroxy-4′-methoxy-pentanoyl-amido-3,6-dideoxy-β-Hex-(1→3)-4-*O*-methyl-α-L-Rha-(1→3)-α-L-Rha-(1→3)-α-L-Rha-(1→2)-6-d-α-L-Tal (Fig. 8B). The serotype 16 GPL should be listed as a group 2 polar GPL in the structural classification of Chatterjee and Khoo (9).

The GPLs of serotypes 7, 12, 17, and 19 have already been classified as group 2 GPLs, which are commonly composed of R→α-L-Rha-(1→3)-α-L-Rha-(1→2)-6-d-L-Tal (R, variable region), possessing a characteristic terminal sugar such as *N*-acyldeoxy-Hex. Indeed, the presence of an amido sugar has been reported in only five GPLs, serotypes 7, 12, 14, 17, and 25 (8, 9, 18). It has been determined that the OSE structure of the

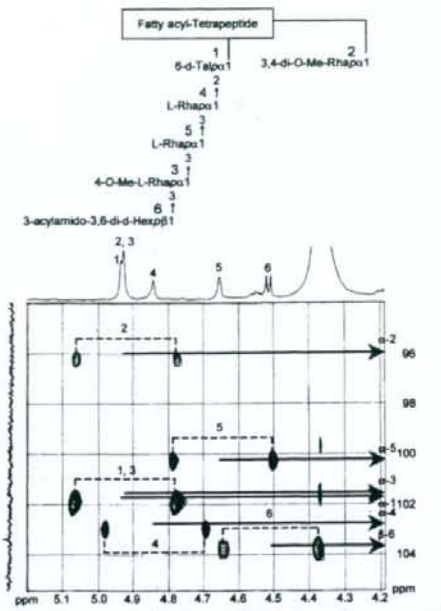

FIG. 6. Nondecoupled ^{1}H-detected [^{1}H, ^{13}C] HMQC spectrum of serotype 16 GPL. Cross-peak labels correspond to those shown on the structure.

serotype 17 GPL was 3-2′-methyl-3′-hydroxy-butanoyl-amido-3,6-dideoxy-β-D-Glc-(1→3)-4-*O*-methyl-α-L-Rha-(1→3)-α-L-Rha-(1→3)-α-L-Rha-(1→2)-6-d-L-Tal (9, 25). Based on the behavior of GPLs in TLC and the GC-MS analysis of alditol acetate derivatives, serotype 16 GPL seems to possess a unique carbohydrate epitope similar to that of serotype 17 GPL. We compared the OSE of serotype 16 GPL to that of serotype 17 GPL. The acylated amido group that was bound to the terminal sugar was different, although the linkage position was identical. Except for the terminal-acylated amido sugar, the other sugar compositions and glycosyl linkage positions were completely identical. An acylated amido group attached to the C-3 position of Hex is very unusual. To our knowledge, 3-amido-Hex is irregular in nature, although 2-amido-Hex is known to be glucosamine or galactosamine, which is frequently isolated as a component of lipopolysaccharides and glycosaminoglycans in prokaryotic and eukaryotic cells (7, 42). Further, existence of short-chain fatty acid 2-methyl-3-hydroxy-4-methoxy-pentanoic acid linked to the amido group of d-Hex is also unique. The characteristic gene cluster is thought to regulate the production of 3-acylated-amido-Hex. It is difficult to determine the species of acylated amido sugars, because no reference standard is available. The terminal sugar of the serotype 17 GPL was reviewed as a gluco-configuration, although firm evidence was not shown (9, 25). The J_{CH} and $J_{1,2}$ values for the anomeric proton in the terminal sugar were 161 and 7.7 Hz,

TABLE 1. Similarity to protein sequences of ORFs in cosmid clone no. 253 derived from *M. intracellulare* serotype 16 strain ATCC 13950^T

ORF	Predicted molecular mass (kDa)	Predicted pI	Exhibits similarity to:	E value	Amino acid identity (no. matched/total no.)	Accession no.
GtfB	45.6	6.35	Glycosyltransferase GtfB	0.0	417/418	BAF45360
Orf 1	45.2	6.10	Putative glycosyltransferase	0.0	416/417	BAF45361
Orf 2	78.9	8.51	Putative acyltransferase	0.0	557/728	BAF45368
Orf 3	31.0	5.88	Putative methyltransferase	2e-89	382/421	NP_218045
Orf 4	15.7	4.94	Conserved hypothetical protein	1e-39	73/129	BAD50406
Orf 5	16.0	4.69	Conserved hypothetical protein	5e-40	75/135	EAX55190
Orf 6	41.1	5.88	Aminotransferase/DegT_DnrJ_EryC1	6e-119	208/357	ABD68440
Orf 7	40.6	9.65	Conserved hypothetical protein	2e-89	178/304	AAS03547
Orf 8	36.7	5.32	Conserved hypothetical protein	2e-52	116/298	CAE06954
Orf 9	22.3	9.79	Putative *N*-acetyltransferase	4e-14	58/166	EAU11841
Orf 10	25.3	7.82	Short-chain dehydrogenase/reductase	7e-47	101/233	EAO61220
Orf 11	23.8	6.05	Putative hydrolase	4e-24	64/196	ABG85599
Orf 12	37.2	6.50	Ketoacyl-acyl carrier protein synthase III	3e-55	126/331	EAX48715
Orf 13	42.5	7.72	Short-chain dehydrogenase/reductase	2e-42	97/248	ZP_01289005
Orf 14	65.8	4.70	Predicted enzyme involved in methoxymalonyl-acyl carrier protein biosynthesis	6e-85	201/575	ABB73590
Orf 15	50.0	6.23	Acyl coenzyme A synthetases	2e-128	233/445	EAT27362
Orf 16	39.1	8.00	Putative glycosyltransferase	2e-106	196/318	NP_855197
Orf 17	37.7	9.46	Putative glycosyltransferase	8e-160	278/323	BAF45369
DrrC	28.6	11.47	Daunorubicin resistance protein C	6e-132	233/261	BAF45370

respectively (Fig. 6; Table S1 in the supplemental material). These results demonstrated unequivocally that the terminal amido-Hex was β configuration and H-2 was in the axial position. The terminal amido-Hex is considered to be derived from glucose or galactose, not Rha.

Next, we explored the genetic mechanism of GPL biosynthesis, because the elongation of carbohydrate chains in serotype-specific GPLs is poorly understood. The *ser2* gene cluster of the *M. avium* serotype 2 strain (31) and a 27.5-kb DNA fragment of the *M. avium* serotype 4 strain (28) were identified to be responsible for the biosynthesis of each OSE in GPLs. Recently, enzymatic characterizations of glycosyltransferase and methyltransferase of nonpolar GPLs have been reported for *Mycobacterium smegmatis* (36, 38). In the serotype-specific polar GPL biosynthesis of MAC, only the *rtfA* gene was functionally clarified to encode the transfer of L-Rha to 6-d-Tal, but which gene cluster transfers the sugars next to L-Rha elongated from 6-d-Tal is unclear.

In this study, we cloned the biosynthetic cluster of the serotype 16 GPL and analyzed its sequence. Seventeen ORFs were detected in the serotype 16 strain, and the sequence homology was analyzed. The transformant of the *M. avium* serotype 1

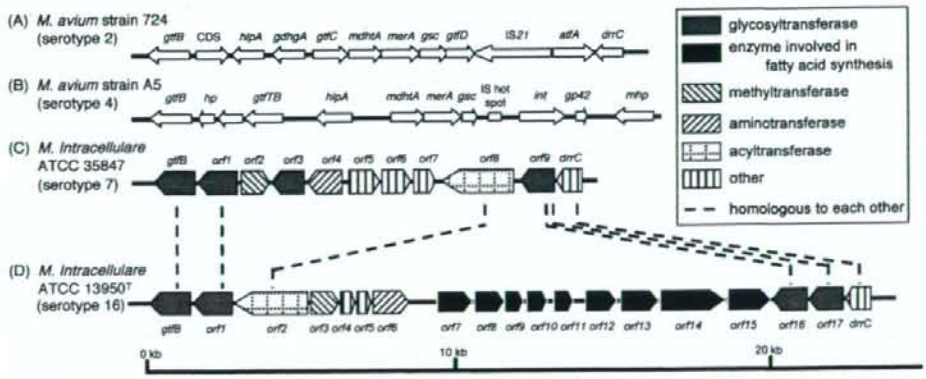

FIG. 7. Comparison and overview of genetic maps of GPL biosynthetic cluster. The *M. avium* strain 724 annotated sequence obtained from GenBank (accession no. AF125999) (A); the *M. avium* strain A5 annotated sequence obtained from GenBank (accession no. AY130970) (B); the *M. intracellulare* ATCC 35847 sequenced in our previous study (GenBank accession no. AB274811) (C); the *M. intracellulare* ATCC 13950^T sequenced in this study (GenBank accession no. AB355138) (D). The orientation of each gene is shown by the direction of the arrow. In panels A and B, putative ORFs not showing homology to known proteins sequences are not depicted. The sequences extending upstream in panels A and B and downstream in panel B are not included in the figure.

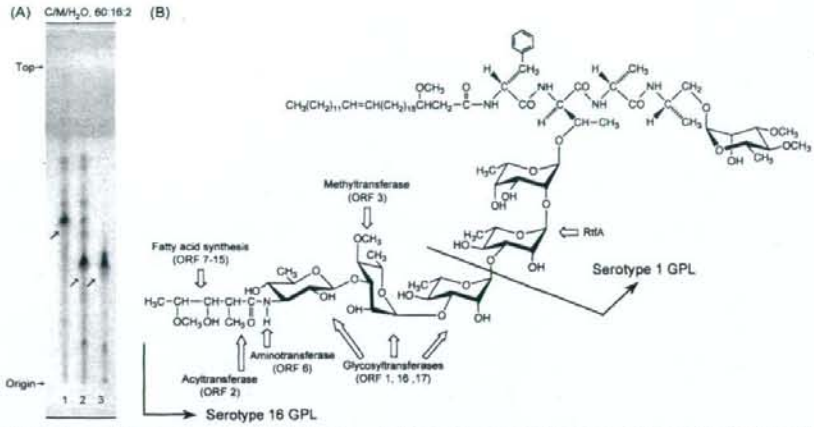

FIG. 8. TLC pattern of *M. avium* serotype 1 and its transformant with cosmid clone no. 253 and proposed complete structure of the serotype 16 GPL. (A) The alkaline-stable lipids derived from *M. avium* serotype 1 (lane 1), its transformant (lane 2), and purified serotype 16 GPL (lane 3) were developed with the solvent system of chloroform-methanol-water (60:16:2, vol/vol/vol). (B) Predicted biosynthesis gene clusters are indicated by arrows.

strain carrying cosmid clone no. 253 produced serotype 16 GPL. These results strongly implied that this *gtfB-drrC* region is responsible for the biosynthesis of the serotype 16-specific GPL. From the structural analysis of the serotype 16 GPL and the sequence of cosmid clone no. 253, it is possible to predict the relationship between the biosynthesis of serotype 16 GPL and the function of each ORF.

The genetic map of the serotype 16 GPL biosynthetic cluster was compared to those of serotype 2 GPL from *M. avium* strain 724, serotype 4 GPL from *M. avium* strain A5, and serotype 7 GPL from *M. intracellulare* strain ATCC 35847^T (12, 18, 28). Significant differences were found in the neighborhood of the conserved region. The genetic organization of the serotype 16 GPL gene cluster was distinct from that of serotype 7, except for some of the ORFs, and the ORFs in this region of serotype 2 and serotype 4 were completely different from ORFs 1 to 17 in serotype 16 (Fig. 7).

In addition to *M. intracellulare* serotype 7 (18) and serotype 16 strains, we have analyzed similar gene clusters of *M. intracellulare* serotype 12 and 17 strains. The sequence homology of the regions of ORF 1 and ORF 17 was highly conserved between only *M. intracellulare* serotype 16 and 17 strains (unpublished data). ORFs 1, 16, and 17 may lead to transfer of the two additional molecules of L-Rha and terminal amido-Hex. ORF 2 was assigned to acyltransferase and may be responsible for biosynthesis of the 3-2'-methyl-3'-hydroxy-4'-methoxy-pentanoyl-amido group in the terminal Hex. ORF 3 is probably responsible for the transfer of the *O*-methyl group at the C-4 position in the third L-Rha from 6-d-Tal. ORF 6 is homologous to aminotransferase and possibly associated with the biosynthesis of an amido group in the terminal Hex. The deduced amino acid sequences of ORF 6 in serotype 16 and ORF 4 in serotype 7 have homologies to DegT_DnrJ_EryC1 aminotransferases. However, these two ORFs are dissimilar to each other. Serotype 16 and 7 GPLs have an amido group at the terminal Hex, although the attachment position is different. The serotype 7 GPL has an amido group at the C-4 position in the terminal Hex, but the serotype 16 GPL has it at the C-3 position. Nine ORFs between ORF 7 and ORF 15 are possibly involved in fatty acid synthesis of the acyl chain moiety linked by an amido bond of the terminal Hex. Taken together, this gene cluster may participate in the biosynthetic pathway of the serotype 16-specific GPL, although further study is needed to clarify the function of each ORF.

Recent studies suggest that GPLs play an important role in the phenotype and pathogenicity of MAC. The colony morphology is considered to be influenced by cell wall GPL. MAC colony phenotypes spontaneously occur from smooth to rough type, and this is due to a mutation lacking GPL (3, 13, 22). The deletion of genomic regions encoding GPL biosynthesis may result in the loss of GPL. Danelishvili et al. demonstrated that the uptake by and growth in macrophages of a MAC mutant with the gene belonging to the GPL synthesis pathway inactivated by transposon insertion were decreased (11). Bhatnagar and Schorey have reported that macrophages infected with MAC release exosomes containing GPLs that result in the transfer of the GPLs to uninfected macrophages and induce a proinflammatory response (4). These findings imply that GPL participates in the pathogenicity of MAC. By contrast, our previous studies have demonstrated that anti-GPL antibodies are detected in the sera of most immunocompetent patients with MAC pulmonary disease and that the detection of anti-GPL antibody is useful for the serodiagnosis of MAC disease (15, 26, 27).

To understand the role of GPLs in MAC and its hosts, it is necessary to define the chemical structure and biosynthesis pathways of GPLs. Elucidation of the structure-function relationship of GPL may open a new avenue for controlling MAC disease.

ACKNOWLEDGMENTS

This work was supported by grants from the Ministry of Education, Culture, Sports, Science, and Technology of Japan, the Japan Health Sciences Foundation, and the Ministry of Health, Labor, and Welfare of Japan (Research on Emerging and Reemerging Infectious Diseases).

We are grateful to Sumihiro Hase (Department of Chemistry, Graduate School of Science, Osaka University, Osaka, Japan) and Hiromi Murakami (Osaka Municipal Technical Research Institute, Osaka, Japan) for helpful discussion.

REFERENCES

1. **Baess, I.** 1983. Deoxyribonucleic acid relationships between different serovars of *Mycobacterium avium*, *Mycobacterium intracellulare* and *Mycobacterium scrofulaceum*. Acta Pathol. Microbiol. Immunol. Scand. **91:**201–203.
2. **Barrow, W. W., T. L. Davis, E. L. Wright, V. Labrousse, M. Bachelet, and N. Rastogi.** 1995. Immunomodulatory spectrum of lipids associated with *Mycobacterium avium* serovar 8. Infect. Immun. **63:**126–133.
3. **Belisle, J. T., K. Klaczkiewicz, P. J. Brennan, W. R. Jacobs, Jr., and J. M. Inamine.** 1993. Rough morphological variants of *Mycobacterium avium*. Characterization of genomic deletions resulting in the loss of glycopeptidolipid expression. J. Biol. Chem. **268:**10517–10523.
4. **Bhatnagar, S., and J. S. Schorey.** 2007. Exosomes released from infected macrophages contain *Mycobacterium avium* glycopeptidolipids and are proinflammatory. J. Biol. Chem. **282:**25779–25789.
5. **Bhatt, A., N. Fujiwara, K. Bhatt, S. S. Gurcha, L. Kremer, B. Chen, J. Chan, S. A. Porcelli, K. Kobayashi, G. S. Besra, and W. R. Jacobs, Jr.** 2007. Deletion of *kasB* in *Mycobacterium tuberculosis* causes loss of acid-fastness and subclinical latent tuberculosis in immunocompetent mice. Proc. Natl. Acad. Sci. USA **104:**5157–5162.
6. **Brennan, P. J., and H. Nikaido.** 1995. The envelope of mycobacteria. Annu. Rev. Biochem. **64:**29–63.
7. **Campo, G. M., S. Campo, A. M. Ferlazzo, R. Vinci, and A. Calatroni.** 2001. Improved high-performance liquid chromatographic method to estimate aminosugars and its application to glycosaminoglycan determination in plasma and serum. J. Chromatogr. B **765:**151–160.
8. **Chatterjee, D., G. O. Aspinall, and P. J. Brennan.** 1987. The presence of novel glucuronic acid-containing, type-specific glycolipid antigens within *Mycobacterium* spp. Revision of earlier structures. J. Biol. Chem. **262:**3528–3533.
9. **Chatterjee, D., and K. H. Khoo.** 2001. The surface glycopeptidolipids of mycobacteria: structures and biological properties. Cell. Mol. Life Sci. **58:**2018–2042.
10. **Daffe, M., and P. Draper.** 1998. The envelope layers of mycobacteria with reference to their pathogenicity. Adv. Microb. Physiol. **39:**131–203.
11. **Danelishvili, L., M. Wu, B. Stang, M. Harriff, S. Cirillo, J. Cirillo, R. Bildfell, B. Arbogast, and L. E. Bermudez.** 2007. Identification of *Mycobacterium avium* pathogenicity island important for macrophage and amoeba infection. Proc. Natl. Acad. Sci. USA **104:**11038–11043.
12. **Eckstein, T. M., J. T. Belisle, and J. M. Inamine.** 2003. Proposed pathway for the biosynthesis of serovar-specific glycopeptidolipids in *Mycobacterium avium* serovar 2. Microbiology **149:**2797–2807.
13. **Eckstein, T. M., J. M. Inamine, M. L. Lambert, and J. T. Belisle.** 2000. A genetic mechanism for deletion of the *ser2* gene cluster and formation of rough morphological variants of *Mycobacterium avium*. J. Bacteriol. **182:**6177–6182.
14. **Eckstein, T. M., F. S. Silbaq, D. Chatterjee, N. J. Kelly, P. J. Brennan, and J. T. Belisle.** 1998. Identification and recombinant expression of a *Mycobacterium avium* rhamnosyltransferase gene (*rtfA*) involved in glycopeptidolipid biosynthesis. J. Bacteriol. **180:**5567–5573.
15. **Enomoto, K., S. Oka, N. Fujiwara, T. Okamoto, Y. Okuda, R. Maekura, T. Kuroki, and I. Yano.** 1998. Rapid serodiagnosis of *Mycobacterium avium-intracellulare* complex infection by ELISA with cord factor (trehalose 6, 6′-dimycolate), and serotyping using the glycopeptidolipid antigen. Microbiol. Immunol. **42:**689–696.
16. **Falkinham, J. O., III.** 1996. Epidemiology of infection by nontuberculous mycobacteria. Clin. Microbiol. Rev. **9:**177–215.
17. **Field, S. K., D. Fisher, and R. L. Cowie.** 2004. *Mycobacterium avium* complex pulmonary disease in patients without HIV infection. Chest **126:**566–581.
18. **Fujiwara, N., N. Nakata, S. Maeda, T. Naka, M. Doe, I. Yano, and K. Kobayashi.** 2007. Structural characterization of a specific glycopeptidolipid containing a novel *N*-acyl-deoxy sugar from *Mycobacterium intracellulare* serotype 7 and genetic analysis of its glycosylation pathway. J. Bacteriol. **189:**1099–1108.
19. **Gerwig, G. J., J. P. Kamerling, and J. F. G. Vliegenthart.** 1978. Determination of the D and L configuration of neutral monosaccharides by high-resolution capillary G.L.C. Carbohydr. Res. **62:**349–357.
20. **Hakomori, S.** 1964. A rapid permethylation of glycolipid, and polysaccharide catalyzed by methylsulfinyl carbanion in dimethyl sulfoxide. J. Biochem. (Tokyo) **55:**205–208.
21. **Heidelberg, T., and O. R. Martin.** 2004. Synthesis of the glycopeptidolipid of *Mycobacterium avium* serovar 4: first example of a fully synthetic C-mycoside GPL. J. Org. Chem. **69:**2290–2301.
22. **Howard, S. T., E. Rhoades, J. Recht, X. Pang, A. Alsup, R. Kolter, C. R. Lyons, and T. F. Byrd.** 2006. Spontaneous reversion of *Mycobacterium abscessus* from a smooth to a rough morphotype is associated with reduced expression of glycopeptidolipid and reacquisition of an invasive phenotype. Microbiology **152:**1581–1590.
23. **Kaufmann, S. H.** 2001. How can immunology contribute to the control of tuberculosis? Nat. Rev. Immunol. **1:**20–30.
24. **Khoo, K. H., D. Chatterjee, A. Dell, H. R. Morris, P. J. Brennan, and P. Draper.** 1996. Novel *O*-methylated terminal glucuronic acid characterizes the polar glycopeptidolipids of *Mycobacterium habana* strain TMC 5135. J. Biol. Chem. **271:**12333–12342.
25. **Khoo, K. H., E. Jarboe, A. Barker, J. Torrelles, C. W. Kuo, and D. Chatterjee.** 1999. Altered expression profile of the surface glycopeptidolipids in drug-resistant clinical isolates of *Mycobacterium avium* complex. J. Biol. Chem. **274:**9778–9785.
26. **Kitada, S., R. Maekura, N. Toyoshima, N. Fujiwara, I. Yano, T. Ogura, M. Ito, and K. Kobayashi.** 2002. Serodiagnosis of pulmonary disease due to *Mycobacterium avium* complex with an enzyme immunoassay that uses a mixture of glycopeptidolipid antigens. Clin. Infect. Dis. **35:**1328–1335.
27. **Kitada, S., Y. Nishiuchi, T. Hiraga, N. Naka, H. Hashimoto, K. Yoshimura, K. Miki, M. Miki, M. Motone, T. Fujikawa, K. Kobayashi, I. Yano, and R. Maekura.** 2007. Serological test and chest computed tomography findings in patients with *Mycobacterium avium* complex lung disease. Eur. Respir. J. **29:**1217–1223.
28. **Krzywinska, E., and J. S. Schorey.** 2003. Characterization of genetic differences between *Mycobacterium avium* subsp. avium strains of diverse virulence with a focus on the glycopeptidolipid biosynthesis cluster. Vet. Microbiol. **91:**249–264.
29. **Maekura, R., Y. Okuda, A. Hirotani, S. Kitada, T. Hiraga, K. Yoshimura, I. Yano, K. Kobayashi, and M. Ito.** 2005. Clinical and prognostic importance of serotyping *Mycobacterium avium-Mycobacterium intracellulare* complex isolates in human immunodeficiency virus-negative patients. J. Clin. Microbiol. **43:**3150–3158.
30. **Marras, T. K., and C. L. Daley.** 2002. Epidemiology of human pulmonary infection with nontuberculous mycobacteria. Clin. Chest Med. **23:**553–567.
31. **Maslow, J. N., V. R. Irani, S. H. Lee, T. M. Eckstein, J. M. Inamine, and J. T. Belisle.** 2003. Biosynthetic specificity of the rhamnosyltransferase gene of *Mycobacterium avium* serovar 2 as determined by allelic exchange mutagenesis. Microbiology **149:**3193–3202.
32. **McClatchy, J. K.** 1981. The seroagglutination test in the study of nontuberculous mycobacteria. Rev. Infect. Dis. **3:**867–870.
33. **McCloskey, J. A.** 1969. Mass spectrometry, p. 402. *In* J. M. Lowenstein (ed.), Methods in enzymology: lipid, vol. 14. Academic Press, New York, NY.
34. **McNeil, M., H. Gaylord, and P. J. Brennan.** 1988. *N*-formylkansosaminyl-(1-3)-2-*O*-methyl-D-rhamnopyranose: the type-specific determinant of serovariant 14 of the *Mycobacterium avium* complex. Carbohydr. Res. **177:**185–198.
35. **McNeil, M., A. Y. Tsang, and P. J. Brennan.** 1987. Structure and antigenicity of the specific oligosaccharide hapten from the glycopeptidolipid antigen of *Mycobacterium avium* serotype 4, the dominant *Mycobacterium* isolated from patients with acquired immune deficiency syndrome. J. Biol. Chem. **262:**2630–2635.
36. **Miyamoto, Y., T. Mukai, N. Nakata, Y. Maeda, M. Kai, T. Naka, I. Yano, and M. Makino.** 2006. Identification and characterization of the genes involved in glycosylation pathways of mycobacterial glycopeptidolipid biosynthesis. J. Bacteriol. **188:**86–95.
37. **Odham, G., and E. Stenhagen.** 1972. Fatty acids, p. 211–228. *In* G. R. Waller (ed.), Biochemical application of mass spectrometry. Wiley-Interscience, New York, NY.
38. **Patterson, J. H., M. J. McConville, R. E. Haites, R. L. Coppel, and H. Billman-Jacobe.** 2000. Identification of a methyltransferase from *Mycobacterium smegmatis* involved in glycopeptidolipid synthesis. J. Biol. Chem. **275:**24900–24906.
39. **Supply, P., E. Mazars, S. Lesjean, V. Vincent, B. Gicquel, and C. Locht.** 2000. Variable human minisatellite-like regions in the *Mycobacterium tuberculosis* genome. Mol. Microbiol. **36:**762–771.
40. **Tsang, A. Y., J. C. Denner, P. J. Brennan, and J. K. McClatchy.** 1992. Clinical and epidemiological importance of typing of *Mycobacterium avium* complex isolates. J. Clin. Microbiol. **30:**479–484.
41. **Wayne, L. G., and H. A. Sramek.** 1992. Agents of newly recognized or infrequently encountered mycobacterial diseases. Clin. Microbiol. Rev. **5:**1–25.
42. **Woods, A., and J. R. Couchman.** 2001. Proteoglycan isolation and analysis, p. 10.7.1–10.7.19. *In* J. S. Bonifacino, M. Dasso, J. B. Harford, J. Lippincott-Schwartz, and K. M. Yamada (ed.), Current protocols in cell biology. Wiley Interscience, Hoboken, NJ.

Jpn.J.Leprosy 77, 29-36(2008)

Leprosy situation in Vietnam - reduced burden of stigma

Pham Dang Bang*[1, 2], Koichi Suzuki[3], Norihisa Ishii[3] and Tran Hau Khang[1, 2]

1)Dermatology Department, Hanoi Medical University, Vietnam
2)National Institute of Dermato-Venereology, Vietnam
3)Department of Bioregulation, Leprosy Research Center, National Institute of Infectious Diseases, Japan

[Received / Accepted: 28 May, 2007]

Key words : elimination, leprosy, stigma, Vietnam, WHO

1. Background

a. Country profile

Vietnam, officially the Socialist Republic of Vietnam, is the easternmost nation on the Indochina Peninsula. It borders China to the north, Laos to the northwest, and Cambodia to the southwest. On the country's east coast lies the South China Sea. The capital of Vietnam is Hanoi and the largest and most populous city is Ho Chi Minh City. Vietnam, with its 4-level administrative system, is divided into 59 provinces and 5 province-level cities, which are further subdivided into districts and municipalities. Each district or municipality consists of 10-20 communes. Often, the Vietnamese government groups the various provinces into eight regions: Northwest, Northeast, Red River Delta, North Central Coast, South Central Coast, Central Highland, Southeast and Mekong River Delta. Vietnam extends approximately 331,688 square km in area. With a population of over 85 million, Vietnam is the 13th most populous country in the world.

b. Leprosy control system

Vietnam's National Leprosy Control Programme was established in 1982. The Leprosy control system had been intergrated into the Health care system which follows the Administrative system (Figure 1). The National Institute of Dermato-Venereology (NIDV) is leading institute responsible to the Ministry of Health (MOH) for skin diseases, sexually transmitted infections (STIs) and leprosy control in the whole country. In each province, there is a Dermato-Venereology Clinic, vertically under the NIDV, covering these three fields at provincial level. Dermato-Venereological activities including leprology work are integrated into general health system at district level. At the district's Social Diseases Unit in endemic zones, several practitioners are specially trained to work exclusively in leprosy field whereas in less endemic district, they are in charge of some contagious diseases such as leprosy, tuberculosis, malaria, HIV/AIDS, etc. In each commune that includes 2-5

*Corresponding author :
Pham Dang Bang. National Institute of Dermato-Venereology, Phuong Mai Street, Dong Da District, Hanoi 10000, Vietnam.
TEL : +84 - 4 - 576 - 4000 FAX : +84 - 4 - 576 - 1649
E-mail :bangphd@fpt.vn

villages with 1,000-3,000 people, leprosy as well as other social diseases are managed by one or two health workers. Because of poor infrastructure at Communal Health Stations, their main work is to refer suspect cases for diagnosis confirmation, to treat and follow up confirmed cases. Antileprosy drugs are stored at any levels, from central to local.

2. Leprosy control activities in the period 1975 - 2006

Dermato-Venereology profession network was established in 1975, immediately after the country's reunion and antileprosy was one of its main responsibilities. A patchy strategy was initially adopted for leprosy elimination activities due to lack of human and financial resources. A total of 21 special projects such as Leprosy Elimination Campaigns (LEC) and Special Action Projects for Elimination of Leprosy (SAPEL) were implemented from 1975, covering more than 2.1 million inhabitants. The projects led to the detection of 1920 new cases and helped clear some leprosy epidemicity pockets, mainly in the central highland and some southern provinces. Because leprosy activities did not cover the whole country, no exact data (prevalence, incidence, etc) was recorded at national level before 1982 but estimated prevalence rate of lep-

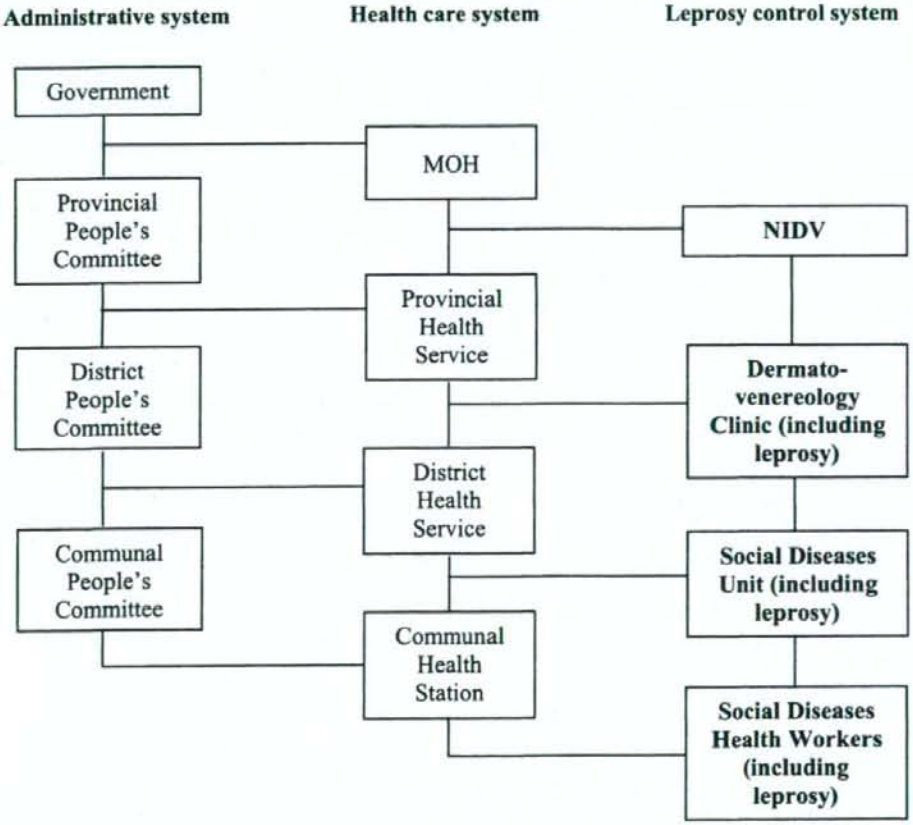

Figure 1. Leprosy control system according to health care and administrative system

rosy was 6 - 7/10,000 population in 1975. Most of patients moved into leprosaria and leprosy villages despite of the fact that there was no segregation law. MDT implementation started in 1983 resulting in dramatic reduction of prevalence rate with nearly 30,000 patients had completed treatment by the year 1995. In early 1990s, leprosy control system was reformed and strengthened with effective supports from international bodies. Thank to effective antileprosy activities, WHO's elimination goal (prevalence rate < 1/10,000 population) was achieved at national level in 1995 (Figure 2) and Vietnam launched its own elimination target of leprosy which are stricter that those were brought out by WHO, including 4 criteria:

- Prevalence rate is less than 0.2/10,000 population in 3 consecutive years
- Case detection rate is less than 1/100,000 population at the time of surveillance
- Grade 2 disability proportion among new cases is less than 15 %
- 20% of community leaders, health workers and high school pupils are randomly chosen for an interview; all of them have basic knowledge on leprosy.

In order to achieve these criteria, following solutions have been carried out:

a. Strengthening the leprosy control network from central to local levels

- extending antileprosy network to all provinces, including provinces with low prevalence rate
- building one referral center for each province or several nearing provinces
- building 3 leprosy and dermatology regional hospitals which are responsible for confirming difficult cases, managing persistent leprosy reactions, doing reconstructive surgery...
- holding retraining courses for leprosy control staff including practitioners, technicians, nurses and village volunteers
- promulgating legislative documents to encourage people working in leprosy field

b. Improving community awareness with IEC (Information, Education and Communication) activities

IEC, as experiences of some countries, plays a

Year	Prevalence rate (1/10,000)
1995	0.70
1996	0.68
1997	0.61
1998	0.44
1999	0.27
2000	0.23
2001	0.20
2002	0.16
2003	0.15
2004	0.10
2005	0.08
2006	0.07

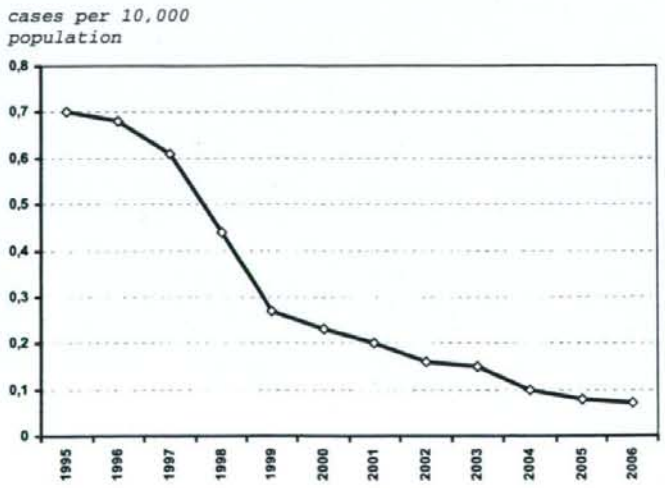

Figure 2. Prevalence rate of leprosy (1995 - 2006)